escola superior de tecnologia e gestão
instituto politécnico de leiria

Thermoforming of Components over Reconfigurable Pin Moulds

Master in Product Design Engineering

Anmol Gupta

Leiria, November of 2021

escola superior de tecnologia e gestão
instituto politécnico de leiria

Thermoforming of Components over Reconfigurable Pin Moulds

Master in Product Design Engineering

Anmol Gupta

Master's Dissertation held under the guidance of Fábio Simões, Professor of the Higher School of Technology and Management of the Polytechnic Institute of Leiria and co-orientation of Artur Mateus, Professor at the Higher School of Technology and Management of the Polytechnic Institute of Leiria.

Leiria, November of 2021.

Originality and Copyright

Dedication

In memory of my grandparents Mr. Om Prakash Gupta and Mrs Sarojini Devi whose love and support were monumental in shaping my life.

Acknowledgements

First and foremost, I would like to express my earnest gratitude to my primary supervisor, Fábio Simões for his knowledge and immense patience throughout my masters program. I would like to convey my thanks to my secondary supervisor professor Artur Mateus for allowing me to contribute on this topic and for offering deep insight into the study.

I am deeply grateful to the research scholars of Center for Rapid and Sustainable Product Development (CDRSP), especially Rúben Silva and Sílvio Póvoa, for their assistance and guidance in experiments. I would also like to thank the international and administrative staff of ESTG for all their help in navigating the higher education system in a foreign country.

I would like to extend my sincere thanks to my best friend Patricio Banda for his help at every stage of this research project. Lastly, I would also like to thank my friends and family for their unwavering support and belief in me.

Abstract

Reconfigurable pin moulds are made of discrete elements that inherently impart surface macro texture when applied to moulding. In this study, the process variables and design parameters were evaluated for thermoforming of plastic sheets using reconfigurable pin moulds, in order to maximize the etched details in the sheet.

Through a qualitative analysis, the effect of the temperature and the amount of vacuum holes in the detail etched was studied for three surfaces with different cross sections and constant area. A DOE model was applied to determine the relationship and correlation between four design factors that were analyzed by using a partial factorial design, whose response was then evaluated on surfaces with different inclinations and height-distance ratios between the pins of the mould bed.

It was found that the combination of a square grid pin bed with an interlayer. Irrespective of the pinhead cross sectional shape and with the curve actuated in a positive setting, produced the highest mean values for the evaluation of the details.

A factor range of 0.939 - 1.05 was determined theoretically for the optimal distance between two adjacent pins where the factor is the arc formed between the two pins divided by the distance between the pins.

Keywords: Reconfigurable pin moulds, Pin heads, Textures, Thermoforming, Multi-point Forming, Flexible Moulds.

Resumo

Os moldes de pinos reconfiguráveis consistem em elementos discretos que transmitem inerentemente uma macrotextura de superfície quando são aplicados para moldação. Neste estudo, foram avaliadas variáveis de processo e parâmetros de concepção para a termoformação de folhas plásticas utilizando moldes de pinos reconfiguráveis, a fim de maximizar os detalhes gravados na lâmina.

Usando análise qualitativa, foi estudado o efeito da temperatura e o número de buracos de vácuo nos detalhes gravados em três superfícies com secções diferentes e área constante. Foi aplicado um modelo DOE para determinar a relação e correlação entre quatro factores de desenho que foram analisados utilizando um desenho factorial parcial, cuja resposta foi avaliada através de superfícies com diferentes inclinações e relações altura/distância entre os pinos do leito do molde.

Verificou-se que a combinação de um leito de pinos formando uma grelha quadrada com uma camada intermédia, independentemente da forma da secção transversal dos pinos e com a curva conduzida numa direcção positiva, produziu os valores médios mais elevados ao avaliar os detalhes.

Um intervalo de factores de 0,939 - 1,05 foi determinado teoricamente para a distância óptima entre dois pinos adjacentes onde o factor é o arco formado entre os dois pinos dividido pela distância entre os pinos.

Palavras-chave: Moldes de pinos reconfiguráveis, Cabeças de pinos, Texturas, Termoformação, Formação multiponto, Molde flexível.

List of Figures

List of Tables

Contents

1 Introduction

Demand in the market is now more dynamic as more consumers prefer customized products and services that are tailor made to reflect their individual tastes and desires. This growing trend has led to a change in the manufacturing environment from long production runs to short volume runs with a larger variety. However, industrial production processes were designed to manufacture large batches of a single product that required dedicated tooling. These rapid changes in product designs makes the mould unsuitable faster and requires a new mould to be made and set up which consumes more time and effort. The introduction of flexible and reconfigurable principles in industrial machines allows for rapid mould redesign, saving resources and reducing labor costs and setup time [1].

Re-configurable moulds are made of elements that can be mixed and matched to customize every product variant. These moulds can be rapidly and repeatedly configured for producing mechanical parts for production. They can be used in variety of processes like forming, moulding and casting to lessen production time and cost. Despite their universality, it has only been applied in cases where a dedicated tooling is not justifiable, due to high cost and storage factors. Pin moulds are a type of reconfigurable moulds that comprise of a bed made of discrete elements called pins. These pins can move in the Z axis to recreate various surface contours. An example of it in commercial application is PinArt toys as seen in figure 1.1. It was first patented by Ward Fleming in 1987 as a vertical three-dimensional image screen [2].

Munro and Walczyk [3] investigated the reasons why this manufacturing technology is not widely used in industrial practice or developed into a commercial product even with the devel-

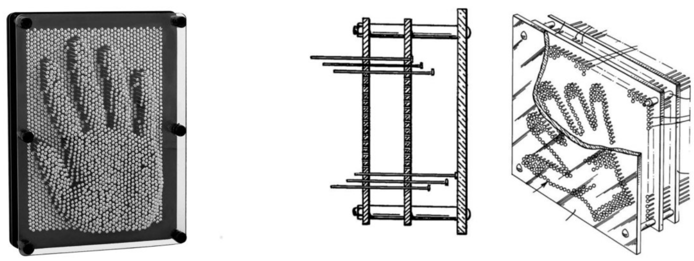

(a) Toy available in the market

(b) As patented by Ward Fleming

Figure 1.1: Pin Art

(a) Adaptive Mould D200 by Adapa used in Architecture [6]

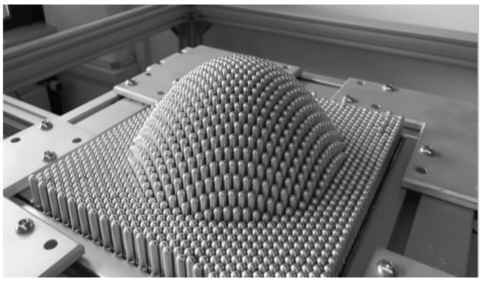

(b) Dynapixel by Cikoni used in Rapid Prototyping [7]

Figure 1.2: Commercial Re-configurable Moulds

opment of new actuation methods and an existing potential market. They suggested it is due to high tool costs, low durability of interpolator surface and advent of additive manufacturing. In their current state, reconfigurable moulds are suited to applications where "part variety is high, production quantities are low and part geometry consists of gentle curvatures".

Munro and Walcyzk also mention Gladwell´s book *The Tipping Point* [4] which postulates three agents of change, one of them is the stickiness factor which in the realm of product design states small details can make products memorable and compel large groups of customers to acquire them. Correspondingly, the subject of this work is to develop a low cost version of re-configurable moulds that does not use an interpolator layer and work together with additive manufacturing to create previously impossible details, that might have the possibility of becoming characteristic of these moulds and open up possibilities of different applications.

1.1 Goals of the work

Mould making industry remains competitive on the basis of three factors, quality, cost and delivery time. Despite rapid development of digital technologies life cycle of moulds is still a major concern [5]. Thus, the concept of re-configurable moulds was introduced in the mould making industry as a potential replacement for conventional tooling. However, till now commercial applications of reconfigurable moulds have been restricted to large scale fabrication of curved composites surfaces where flexibility and size are prized over surface requirements, as seen in figure 1.2.

In reconfigurable pin mould, the mould surface is discretized into smaller individual elements of a particular size with the freedom to move in the Z axis. This lends versatility to this process, but is also the reason for two major limitations which significantly impacts the parts that could be manufactured using this technology [8]:

- dimples caused by the pins in the part surface

- cross sectional size of the pin and the arrangement of the pins

Prior research has been focused on developing smoothing techniques to minimize the dimples caused by the pin based tooling to match the quality from a conventional mould. To that effect, a rubber interpolator layer is introduced to provide a smooth surface for the plastic to form on. This in turn creates parts without any details [9] [10]. It is proposed that instead of looking at reconfigurable pin moulds as substitutes for conventional tooling and focusing efforts on minimizing these perceived surface defects, this geometric waviness can be considered as inherent part of the process and maximized as an aesthetical or functional feature in new applications. For example, this technique could be employed to create textured panels or to manufacture pleasing packaging.

Based on this preliminary understanding, the research objectives are listed as follows:

- Research objective 1: Understand the advantages and limitations of using the pin tool in thermoforming.
- Research objective 2: Design pin attachments for re-configurable pin moulds and analyse the surfaces produced.
- Research objective 3: Propose a set of parameters that produce high quality surfaces with maximum details and applications where such surfaces and reconfigurable moulds could be used.

1.2 Methods and techniques

This study will present mix methods research integrating both qualitative and quantitative research. This approach of combining and analysing the statistical data with deeper contextualised insights is used due to the subject matter texture being highly subjective. After conducting the literature review, design and process parameters will be tested to gauge their effect. The resulting surfaces produced will then be analysed to gain a set of optimized parameters.

1.3 Outline

The work presented in this thesis is divided into four chapters. The current chapter introduces the concept of reconfigurable moulds, the relevance of the subject and gives an overview of the objective of this research. The second chapter goes into an in-depth review of re-configurable moulds by surveying the literature available and then briefly discusses basics of thermoforming and the combined application of these two technologies to identify possible research opportunities in creating textures. The third chapter explains the methodology that was used in experiments to understand the capabilities of the pin tool prototype in the thermoforming setup and the design of reconfigurable mould attachments. The fourth chapter analyses the results of the experiments and discusses possible applications. The fifth chapter summarises the most relevant findings with future research directions.

2 Literature Review

In the following chapter reconfigurable pin moulds are introduced. In addition, their functionality, components and actuation mechanisms for different applications are explained. Next, thermoforming technology is discussed with sections on process, moulds and materials. Lastly, the benefit of textures and different type of patterns is explored and how they are utilized in different industries, like packaging, architecture and design, among others. The objective of this discussion is to identify recent stage of developments in these three subjects and explicate by what method reconfigurable pin moulds could be be used to include texture in new thermoforming applications.

2.1 Re-configurable moulds

Re-configurable moulds are not a new technology, as they have been around for at least 150 years [3]. Yet there is no standardized set of terminology, the keywords used widely differ. Some recurring terms used to refer it are variable geometry mould, reconfigurable tooling, pin bed tooling, discrete dies, flexible moulds, free form fabrication so on and so forth. In this thesis, customisable moulds will be referred as reconfigurable pin moulds. This term encompasses the flexible nature of these moulds without focusing on specific features like geometry, actuation etc. The term details will denote the outline of the pinheads.

> "A reconfigurable tool is defined as a machine that can be repeatedly configured by a user for shaping mechanical parts in a manufacturing setting. Despite being flexible and enabling companies to save time and money, these have still not been adopted by industries and are only found for niche practices." [3]

Re-configurable tooling primary application has been thin shelled surface generation rather than 3D solid object manufacture. It can be reshaped repeatedly by vertically repositioning each element resulting in new surface geometries. Geometric algorithms in this technology are highly efficient and have been used for the planning operations [11], surface approximation, error estimation, pin obstruction [12], [13] and reverse engineering [14].

2.1.1 Components

Re-configurable moulds are based on the discretization of the mould surfaces into a number of elements that can be positioned in the vertical direction. This positioning can be done by a variety of methods as described in the next section. Tooling characteristics of reconfigured moulds are divided into three main parts: pins, interpolation layer and the beds.

Pins are adjustable units that give rise to the so-called reconfigurable pin-type tooling, tools that allow to generate surfaces of variable geometries by reshaping the pins, in a manufacturing setting [10]. Pins have the following set of features and parameters:

- Pin Dimensions - Pin size and height determines the resolution of the matrix. A matrix with higher resolution can create a product with finer level of details and extensive depth. However, there is a trade-off between minimum pin size and maximum pin height vs manageability and costs [15].
- Pin Shape - The body of the pin can have different uniform polygon cross-section such as square, hexagonal, circular, triangular etc. Selection of pin shape can depend on their usage for example cylindrical pins are used for their ease of use during manufacturing while square pins can be closely packed.
- Pin Density – Pins can either be closely packed or uniformly spaced. Greater the number of pin, more duplication of effort is required. The packing can be uniform or non uniform, but former is preferred as varied spacing can lead to complications.
- Resolution - Spatial resolution describes how small an area of the surface can be manipulated. Displacement resolution is a measure of how finely the position of the pins can be controlled [16].
- Pin Configuration - The pins are placed along a grid, covering spatial positions that when put together can form different geometries as shown in 2.1 , square and triangular are the most used as they are the basic shapes that can give rise to more combinations, depending on the need of the application.
- Pin Heads - The pins can be capped with different types of heads depending on the interaction with the part. The end of pins that form the surface can be spherical, square, conical etc. They could also be specialised to perform functions such as fixturing, molding etc. The ability to exchange pinheads allows greater freedom for the pin tool.

Interpolation Layer is a layer of commonly flexible material that is placed between the pins and the material to be manufactured, for example, neoprene. Its main function is to provide a surface in order to limit the waviness in the formed surface [17].

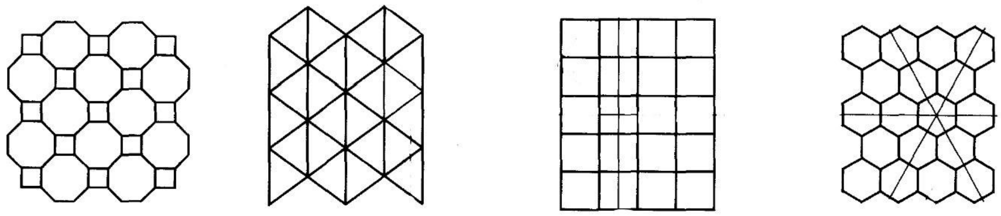

Figure 2.1: Pin Cross Sections - *From left to right* Octagonal & Square, Triangular, Square, Hexagonal

Pedersen and Lenau experimented with different interpolator thicknesses for dimple suppression to level out the mould surface. They found out that the depth of the dimples is reduced as the thickness of the interpolator is increased but that also results in low fidelity of details [10].

2.1.2 Actuation Mechanisms

Re-configurable moulds can be actuated by variety of mechanisms, ranging from manual to automatic. Pins can be moved to their required position in a specific mould manually or automatically.

The simplest method pins can be actuated is manual adjustment through the use of lead-screws as seen in figure 2.2 (b) that have the advantage of self-locking and self supporting when a thread with the right pitch is used as demonstrated by Pedersen and Lenau and Im et al. This method is valid for applications where forming loads are low and tolerances are high but it requires a large a mount of time for positioning and verification. Berteau [19], even patented a design where threaded pins are closely packed, and to be actuated, the pin has to be rotated about its axis, sliding longitudinally using the threads of the adjacent pins.

The positioning of the pins can be done by a numerical controlled machine and ultrasonic vibrator to push a metal tool towards the pins either one at a time or in multiples doing a sweep. The curved surface can also be generated alternatively using a master model [20]. Both methods are shown in figure 2.3(b).

Haas et al as seen figure 2.2 (a), described a shaft-driven lead screw concept where the pins are made of steel tubes with a lead screw inserted in the core. The lead screw is rotated when the clutch is engaged using a worm gear. This actuation method can position with sufficient accuracy with timing, to eliminate the need of position sensing device for each pin.

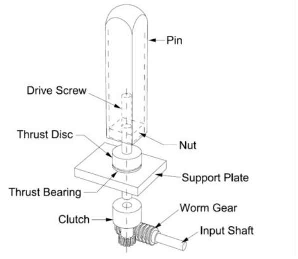

(a) Actuated by an Input Shaft-Worm Gear-Clutch Drive Train [21]

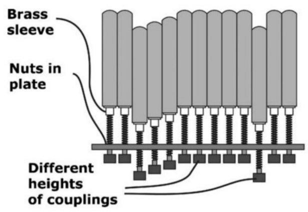

(b) Actuated Manually [10]

Figure 2.2: Examples of Actuation Methods

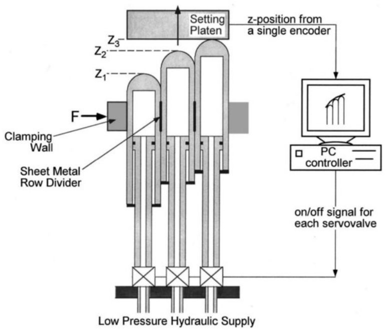

(a) Actuated hydraulically [22]

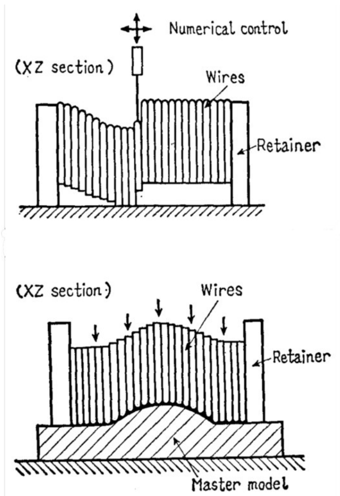

(b) Actuated by CNC machine or a master model [20]

Figure 2.3: Examples of Actuation Methods

However, the clutch is the weak point in this design [21].

Walczyk and Im [22], as seen in figure 2.3(a) demonstrated viability of hydraulically actuated pins. The advantage is there is only one power supply, making it mechanically simple. Two systems were tested, in open loop mode position is controlled by timing the constant-velocity, tracking the upward movement of individual pins until a prescribed position is reached and the closed loop mode with the help of position sensor which makes the system much more complex. However both options have low position accuracy and repeatability.

Using the same packing configuration as the Humphrey design[23], Paul used a combination of two robots to divide the actuation process into two steps, roughing pass and the finishing pass. The first manipulator actuates the pins to their height positions and the second manipulator shapes the pin ends into a more smooth, sculpted surface [24]. Apart from positioning the pins, robots can also be used store, transfer and arrange the pins into producing the mould as described by Todoroki [25]. Kaufman also describes a simple setup using robotic arm to form composites [26].

Moulds can also be actuated interactively and more intuitively by employing variety of input methods, that can be switched with one another, during the process itself. As shown by Protomoulds [27], the user can alter the height of each pin with hand gestures or can draw the outline of the mould directly on the plastic sheet with a whiteboard marker where a camera detects the line and the pins located inside the outline are then raised to press against the plastic and form the shape. They can also use traditional scanning data through the inbuilt camera or manipulate using the virtual model of the pins available with the accompanying software.

2.1.3 Applications

Reconfigurable pin type tooling has been used in different areas of industrial application, its versatility when adapting to new applications is shown in the following 6 areas where projects are being implemented with this technology.

- Forming - Re-configurable tooling have been applied in the field of sheet metal forming for automotive, airplane, and locomotive industries [28–33]. Humphrey later on suggested the use of an interpolation layer which is a flexible membrane placed over the pin surface to prevent any material leakage, smoothing out the surface and easing demoulding [23]. This allowed the technique to be applied for plastic sheet forming. Thus, Kleepsies and Crawford were the first to apply reconfigurable moulds to the thermoforming process and present the waviness problems [34].

- Moulds - The trend in the construction industry to create organic, fluid shapes and forms in architecture are time and labor intensive. New production methods using reconfigurable moulds provide an efficient method to create custom mould surfaces that are non standard and complex with less effort and wastage. Materials such as concrete facade panels that are double curved can either be cast in the flexible mould system itself [35], or cast in a secondary form work that utilizes the geometry formed in the system [36], where two vacuum formed plastic sheets with the desired curves were held vertically and reinforced on either side to create a counter pressure on the poured concrete.

  Other popular materials that are used in architectural projects are composites and sheet metal [37]. Different configurations of reconfigurable surfaces have been used to fabricate non repetitive, irregular geometries in textile composite panels [38], glass fiber reinforced concrete [39], bending glass [40], and sheet metal panels [41].

  Narisco created a moulding device for solid form generation and tested the concepts for forming resin-infused carbon fiber composites and bone replacement geometry. She

(a) ShapeCAD Project [49] **(b)** Transform Project [50]

Figure 2.4: Reconfigurable moulds as Interface

observed flash or excess material is observed on the moulded object at the interacting edge and stepped effect on the surface finish [42].

Zah and colleagues developed a form flexible to make injection moulding for small objects more economical. For such 3D applications a clamping device and closed pack configuration becomes necessary to prevent relative movement of the pins and any leakage of the liquid plastic [43].

Koc building upon the work of variants of Kelkar et al. introduces several methods to increase the structural rigidity of the component by using constraints. This lead in tool strength can prevent gap formation in worst case loading during solid form generation moulding activities [44]. Hong patented a four sided moulding mechanism that can be used to creates gypsum or plaster moulds of people [45].

- Fixturing - This can be seen in the development of reconfigurable and flexible fixturing devices that can be re-positioned to conform to a wider variety of parts and products. This is achieved by employing actuators and measuring devices either placed internally or externally. These methods of adjustment can range from manual to automatic and are selected based on the manufacturing conditions and financial analysis of the process [46]. Park et al. [47], present a transformable pin matrix fixing system that allows to automatically set the optimal pin height in order to reduce the deformation caused by the positioning failures of the automotive doors that go through the assembly process of the ultrasonic welding and screwing.

- Interface - Reconfigurable technology has an immense potential for creating interactive displays in exhibitions. Project Feelex created a technique that combined visual and haptic sensations. This was accomplished by connecting an actuator array to a flexible screen onto which images could be projected. The user could deform the screen by touching and depending on the location and the amount of force applied, the recorded graphics appear to be in motion [48].

  Similarly, reconfigurable components are also applicable to the field of Human-Computer interaction (HCI). They can create dynamic pathways that instruct users on the actions they can take. The inForm system is a shape changing interface that renders physical UI elements on the basis of programmed states. These affordances can transform in shape, size, location, orientation and also appear or disappear on command enhancing the previously static nature of physical objects. The feedback is tracked using an overhead depth tracking camera [50]. Another project by the same lab explores how these mould can improve our interactions with day to day objects for example an augmented phone case as seen in figure 2.4 (b).

Another iteration of shape displays using reconfigurable technology is ShapeShift. It builds upon previous work but goes further by rendering spatial tracking data with a smaller mobile tabletop array. This kind of self actuation can give a tangible dimension to virtual reality applications [51]. Tactile shape displays increase accessibility in blind and visually impaired users to design, produce and edit 3D models with real time haptic feedback [49] as seen in figure 2.4(a).

Large scale pin type tooling have been used as building blocks for prototyping room-scale shape-changing interfaces. These modular, inflatable actuators are low cost, highly extendable and support up to 10 Kg load. These constructive tiles can be used for a variety of scenarios like pop up furniture or information displays [52].

In the same vein, different projects from MIT Media Lab have demonstrated how reconfigurable moulds can be used as adaptive and dynamic table to support a variety of physical activities [53], or used as an abstract storytelling medium [54], or allow interaction with music in real time by manipulating sound waves [55]. Inspired by the Feelex, NSF Digital Clay project is a project conducted in GIT Atlanta focused on the design of a physical graphical user interface (GUI) and output device capable of changing surface shape in response to the pressure applied by human hands or by a 3D model [56], [57].

- Scanning - Generally, reconfigurable pin tooling systems are set up with 3D CAD models but recently advances have been made where a set of digitized points obtained from reverse engineering can be converted into NC tool paths for rapid reproduction. This can be achieved using geometric algorithms that treat the data to determine approximation of NURBS surfaces and eliminate any error [14].

  Tam and Chan demonstrated a novel scanning approach system using pin array digitiser and a smoothing technique, by reverse engineering the part surface to generate a point cloud which is then segmented and treated to satisfy draw ratio, demoulding and strengthening aspect of a thermoforming mould [58]. This approach saves costs and illustrates another utilization of reconfigurable pin moulds.

- Casting - Recently the reconfigurable technology has been applied to the casting industry to mark green sand castings with unique identifiers that allow traceability while significantly decreasing process cycling time. The study developed an insertion tool made of paraffin-graphite blend that got activated with electrical flow. As the current passes, the tool gets heated due to resistance, expanding the paraffin, thus raising the marker [59].

A review of works done by other researchers in vacuum forming [8], [34], [60–62], illustrate that the main focus was on creating surfaces that had a smooth interface. The application of reconfigurable moulds to the thermoforming process is considered as this is a sheet forming process that uses relatively low temperature and pressure. The moulds used can be made of materials such as wood or plastic that are easily workable. This in addition to the use of manual actuation techniques would allow faster and easier development of a prototype. The materials used to test to validate the process are also more economical compared to other process. Hence, the manufacturing process chosen for the experimentation is thermoforming

2.2 Thermoforming

Thermoforming is defined as a secondary moulding technique process where a plastic sheet is shaped using heat and pressure. Thermoformed products can be classified into two main categories: disposable products and industrial products. Industrial products are durable and built to last. They are made of thick gauge plastic sheets like panels and liners in transportation and appliance industries. Disposable products which have shorter life expectancy are formed from thin gauge plastic rolls. For example blister packs, single use cutlery, protective plastics casings etc., are mainly used in rigid packaging and pharmaceutical industry [63–65]. Examples of thermoformed products can be seen in figure 2.5.

According to PlasticNews in 2020, 85% of all thermoformed products are disposable products and the production of these items is very fast and carried out in large quantities. [66] The growth in the industry is fed by on demand lifestyles as the market has shifted toward e-retailing channels and convenient packaging. Manufacturers are looking for bio-based options to meet this rising trend by using biodegradable plastics such as PLA (Poly Lactic Acid) to produce sustainable packaging without changing the process and equipment [67–69].

Thermoforming technology is also an highly efficient method for creating composite structures such as FRP (Fibre reinforced plastics), WPC (wood plastic composites), etc that combine the desired properties of its building components resulting in superior multi-layer laminates that are only required for small scale runs [70–72].

2.2.1 Process

Thermoforming is a secondary, one side forming process. The production starts with extruded sheets which can be single or multi-layered with different grades, colours and additives for versatile properties. Thermoforming process converts these sheets into different forms and shapes by following a five step process:

(a) Disposable products

(b) Industrial Products

Figure 2.5: Thermoformed Products

- Loading - Sheets are classified by their gauge as referenced in table 2.1. Thinner sheets are handled as continuous rolls while thicker gauges are cut into the proper size and stacked flat. Forming sheets above 13 mm are generally not included in this process. The sheet is then held securely in a clamping mechanism.
- Heating - The sheet is heated uniformly using radiant heating elements until it reaches its forming temperature window. This can be observed when a sag in the sheet is visible. Heating of the sheet takes the longest time in the cycle, this time can be reduced with the help of localized and rapid ultrasonic vibration energy [73].
- Forming - When the sheet touches the mould surface, it is chilled and stops stretching. As stretching continues, the sheet free of the mould surface gets thinner and thinner. The part of the sheet that is formed last is the most weak and oriented section. This differential stretching results in non-uniform wall thickness.
- Cooling - The sheet is allowed to cool to a temperature where the new shape will be sustained. The cooling process can be quick or slow depending on the mould material and part thickness.
- Trimming - Part is removed and then the excess material is trimmed and recycled. In some machines the trimming is done before the part removal. At other times, the part is filled and sealed for example in cups, or capsule packaging.

It is important to note for our objective that during the cooling process the sheet increases its density and shrinks in the opposite direction to the external walls of the mould, so in theory it is possible to generate structures that have walls with zero draft angle (angle that is formed between the parallel to the wall and horizontal to the base). However, this is not recommended because such angles can lead to holes, very thin walls, webbing, and severe sidewall thinning. Normally moulds have draft angles ranging from 1-5 degrees and it is recommended to place the highest possible value that does not compromise the other parts of the design [64].

On the other hand, the corners are points of great concentration of effort, and depending

Table 2.1: Sheet Classification by Gauge

Types of Sheets	Gauge
Film or Foils	$<$0.25 mm
Thin	0.25 - 1.5 mm
Mid	1.5 - 3 mm
Thick	3 - 13 mm
Plates	$>$13 mm

on their location, internal or external, and the number of planes that intersect, 2D or 3D, their reproduction will depend on how sharper they are. The sharper it is, the thinner and weaker the part will be at that point. It is therefore recommended to increase the radii or corner chamber to minimize these problems [74].

2.2.2 Thermoforming Parameters

In this section the various parameters related to thermoforming are discussed.

Moulds A thermoforming mould must fulfill the following criteria from creating a part according to specifications [64]:

- A dimensionally stable surface against which a formable plastic sheet can be formed.
- It should allow for the removal of heat from the sheet, repeatedly and efficiently.
- It should be robust enough to withstand repeated forming at elevated pressures and forming sheet temperatures.
- It should withstand corrosive gases from plastic, erosion and wear from filled or reinforced plastic and should survive environmental conditions during long term storage. It should be repairable if damage does occur.

Part Design In a mould, each structure and geometry has its peculiarities, here are some general considerations to be taken into account when designing parts for thermoforming.

- the uniformity of wall thickness;
- corner strengths;
- ability to stack;
- structural stiffness and mechanical response of the structure;

- material consumption;

The design parameters that most affect the thickness variation of the sheets are draw ratios, which are a set of measurements that allow comparing figures with different geometries. Aerial Draw Ratios (ADR) determines the overall stretch measurement of the sheet, by dividing the surface area of the formed part by the surface area of the sheet used to form the part. Linear Draw Ratios compares the length of a straight line drawn on the sheet before forming as compared to the length of the same line after forming, in order to evaluate the tool and define if it is better to use a cavity or plug mould. Height-to-Dimension Ratios which evaluates the symmetry of the shape by the ratio between the height of the formed part divided by the length of the greatest opening of the part [65].

Conditions The sheet thermoforming process is widely used in the industry because of the friendly operating conditions that the process demands. Forming pressure ranges are generally below 14 psi and up to 150 psi depending on the forming method used [65]. It is not necessary to reach the melting temperature (Tm) of the material in order to form it, unlike moulding. This process takes place in the range between the value identified as lower limit forming temperature that corresponds to the heat deflection temperature (HDT), temperature at which the material begins to soften and starts to be malleable, effect generated by the release of its secondary molecular bonds of attraction and the upper limit forming temperature that is located below the Tm range known as thermoforming window [35].

Features Thermoforming technology has a distinct advantage over other plastic processes when it comes to texture, as it picks up minute textures. There are two ways textures and patterns can be incorporated in any thermoformed product: First it could pick up the texture from an etched mould surface or the extruded sheet itself could be formed with having an embossed surface. Once a mould has been etched its very difficult to have it modified, this is because modified moulds can affect the fit and tolerances of the product resulting in errors. However using a textured sheet is possible because unlike other processes the cosmetic side of the sheet, doesn't come into direct contact with the mould surface. Table 2.2 defines some of the features of both options. Some of the most prevalent textures can be seen in figure 2.6, [75].

2.2.3 Thermoforming Material

Within the thermoforming process, the most widely used materials are thermoplastics. Those polymers that have the ability to melt and become moldable again even after they acquire their solid state. Some of the most commonly used thermoplastic polymers for thermoforming of sheets and surfaces are presented in table 2.3.

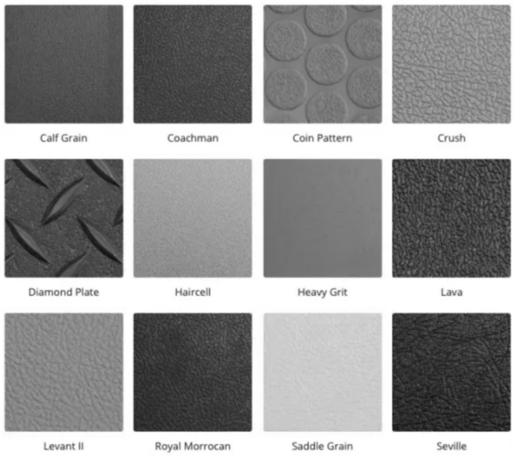

Figure 2.6: Textures in Thermoforming

Table 2.2: Texturing options in thermoforming

Options	Features
In mould textured surface	Texture can be etched into the mould in defined patterns and areas Greater texture detail and depth than other moulding processes Contrasting surface finishes for variation and high level of details Difficult to modify the mould once formed Multiple texture options are available Texture formed directly into the finished part Functional design features can be added
Pre textured plastic sheet	Lower tooling cost than in-mould texturing Minimal texture pattern options Fewer details than in-mould texturing Texture depth variation over the part surface Pretextured sheets available from suppliers

Table 2.3: Thermoforming Temperatures [64]

Polymer	Forming temperature (°C)	Forming temperature range (°C)
Polystyrene (GP-PS)	149	127–182
ABS	166	127–182
Rigid PVC	138	104–154
Acrylic (PMMA)	177	149–193
Polycarbonate (PC)	191	168–204
HDPE	146	127–182
Polypropylene (PP)	154	132–166
APET	149	121–166
40% GR PP	204	129–232

Below is a list of the most used thermoplastics. Along with their main characteristics, new studies are included that showcase development of sustainable alternatives. This in most instances is achieved by extending the useful life of the materials by the formation of composite materials.

Polystyrene General Purpose Polystyrene (GPPS) is an amorphous thermoplastic with a wide forming window, it presents a transparent appearance and has a high modulus, a low room temperature elongation at breaking. Material with great acceptance in the disposable and packaging industry mainly due to its low cost and ease of thermoforming. Its main disadvantage is its high rigidity and fragility, which can make trimming difficult, leading to micro-fractures that can spoil the thermoformed part. Different materials have been added to increase the impact resistance of PS, being butadiene the most common and giving rise to high impact polystyrene (HIPS) [64], [65], [76].

Kaho et al. [77], presents the fabrication of a mixture of expanded polystyrene (EPS) and wood waste, for which a solution made from EPS dissolved in acetone is used as homogenizing resin. As a result, the thermoformed samples were less porous, more homogeneous and absorbed less water than the non-thermoformed samples.

Acrylonitrile butadiene styrene (ABS) An opaque amorphous polymer is a versatile polymer which combines the properties of the three elements that make it. It preserves the processing ease of styrene, and combines the gloss and weatherability of acrylic with the impact resistance of a synthetic rubber such as butadiene. This is used when high impact strength is needed yet transparency is not required, such as appliance cabinets, medical devices or shell housings [64], [65], [76]. Sanguanwong et al. [78], elaborated a mixture of different thermoplastic polymers including recycled ABS, in different proportions for use as a composite material in the formation of interior structural products for automotive industry, achieving satisfactory results.

Polyvinyl chloride (PVC) A hard, rigid, translucent polymer. Its composition makes it a fire-retardant with a limiting oxygen index (LOI) greater than 30, which is why it is used in transportation or electronic equipment coating applications where flammability ratings may be an issue. It is sensitive to overheating, presenting color shift or discoloration. If the by-products of excess heat in the process are mixed with water, it can generate hydrogen chloride (HCl) gas due to its chemical composition thus, additional safety precautions within the thermoforming system are required [64], [65], [76]. PVC is incompatible with several polymers, having some affinity for acrylates.

High and Low Density Poly Ethylene (HDPE / LDPE) Low cost crystalline thermoplastic, with density around 960 kg/m^3. It serves as a barrier for the passage of water vapor, characteristic that makes it one of the preferred materials in the food packaging industry, together with its low density presentation (LDPE). HDPE has as main characteristics a high impact strength, chemical resistance, and excellent outdoor weatherability, having applications in the formation of pallets, marine and garbage cans. LDPE, on the other hand, has a much lower modulus than its high-density counterpart, a property that gives it the flexibility necessary to be useful in the flexible packaging industry [64], [65], [76].

Several studies have been conducted in the quest to extend the shelf life of single-use disposable plastics and flexible food packaging. Awoyera evaluated the feasibility of using polymer blends, including LDPE and HDPE materials recovered from the sea, in the production of composite cements, achieving at the end of its work to prove the ability to use these wastes as secondary raw materials in a new production process [79].

Polylactic Acid (PLA) & Green Polyethylene (PE) Special mention must be made of biodegradable polymers and composites. Polylactic acid is a crystalline polymer with a glass transition temperature between 55°C and 65°C, density of 1.25 g/cm^3 and highest modulus of elasticity at 3500 MPa. The physical properties of PLA can be improved by material orientation, for example bi-axially oriented sheets. It is a renewable thermoplastic obtained entirely from corn and can also be produced from other renewable resources that contain natural plant sugars such as sugar beets, wheat etc. It biodegrades by hydrolysis, so it must be protected from moisture in the air. PLA is suitable for applications ranging from soft drink glasses, fruit and vegetable trays, and refrigeration and freezer containers [80]. Green Polyethylene made from sugar cane is as an alternative to regular fossil based polythene with the same properties as PE but renewable and sustainable. It is not biodegradable like PLA but can be recycled. Altinbalik studies how green PE can be used in the thermoforming process to achieve the same result as traditional PE [81].

2.3 Textures and Patterns

2.3.1 Texture

Perception of texture can relay information through visual, acoustic and tactile communication. In common terms it is the feel or appearance of a surface. The use of physical and visual textures in design can convey a variety of emotional responses and functional behaviors. Every texture has its corresponding personality trait that originates from learned expectations from the natural environment and can trigger clues in the built environment.

For designers it is a powerful tool that remains invisible to the viewer unless it doesn't align with their expectations. In engineering, surface texture can enhance properties of materials with top (cutting, etching, grinding) or bottom (deposition, coating) processes. Coblas and Moronuki [82], reviews surface texture manufacturing methods (nano to micro scale) and how they have been applied in various fields such as optics, physics, bio-medicine, tribology, energetics, electronics, metrology. The design of functional texture if often inspired by natural designs [83]. However, the objective of this thesis will be focused on macro textures and their functional and aesthetic features.

Texture in Architecture and Interior Design In architecture and interior design, textures can stimulate pleasant psychological associations in an interior space with the help of biophilic designs. These imitations of natural forms and elements in the built environment can nurture cognitive well being [84]. They are also effective tool for creating mindful spaces as different types of textures interact with light in their own way. Furniture and furnishings with smooth and shiny fabrics such as silk and satin reflect more light giving an extravagant appearance while rougher fabrics such as fur and wool absorb or diffuse lights creating a warm and cozy environment. Combination of textural contrasts can be used to either balance or highlight lighting in any room [85]. Similarly in product design, physical and visual textures trigger feelings of elegance and class with smooth, high gloss finishes, or strength and industrial responses from rough or hard finishes.

Spence and Ferreira review how tactile textures implemented in packaging designs can significantly affect the consumer perception and behavior towards the product itself and the need for texture compatibility between product and packaging for a positive impact [86], [87]. A study conducted in Brazil with visually impaired people suggests inclusive models to design accessible packaging that provide tactile details about opening and closing of the package, expiry date of the product, nutritional information and brand identification [88]. Braille is one way to make packaging accessible, but it is not as commonly used. [89] Raised symbols and QR codes as seen in figure 2.7 are great examples of inclusive designs that enhance usability for all customers.

Texture in Product Design Texture in food science and technology has emerged as one of four key factors that form the eating experience and can even determine appreciation and acceptability of food items. It is an integral sensory component with multi parameters that can be modified to enhance the textural profile using food processing techniques [90–92]. One of the common applications is the use of silicone food moulds to make puree foods more attractive to patients with dysphagia [93] and to influence food preferences in young children by promoting tactile exposure [94].

Texture also has various tribological applications. A study conducted by worobets et. al presented that maximizing traction on the outsole of running shoes resulted in increased

(a) VictoriaLand Beauty´s Packaging

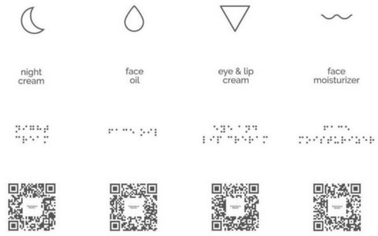

(b) Universal Raised Symbol's 2

Figure 2.7: Accessible Packaging Example

(a) Slip Resistant Crocs with raised surface area

(b) Colgate 360º Manual Toothbrush

Figure 2.8: Everyday examples of tribological applications

performance in the athletes [95]. Textured thumb grip in Colgate 360º manual toothbrush improve stability and handling of the brush during activity. Both examples can be seen in figure 2.8, [96]. Similarly, it is possible to find the use of macro textures in dumbbells, handlebars, coffee cup grips for slip resistance and ergonomics.

Texture in Packaging Design In thermoforming packaging products, flat surfaces are avoided, as the slightest distortions are manifested and the part will lose its quality appearance. Rounding, arching of surfaces or incorporating high reliefs, ridges and grooves increases the rigidity of the formed part and allows the use of thinner sheet materials. Not only reducing overall cost but also being eco-friendly by minimizing consumption of plastic. These effects protect the contents of the packaging [76].

Rodriguez-Parada, Mayuet, and Gámez studied how mechanical properties of thermo-

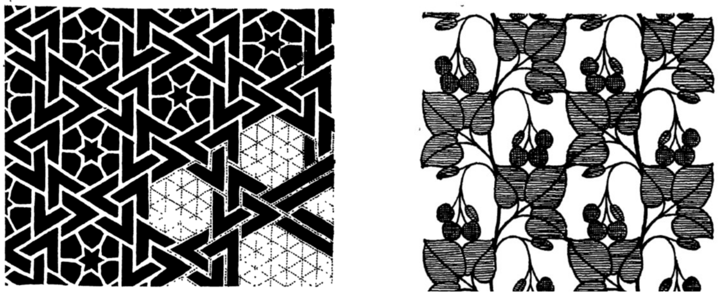

(a) Geometric Lattice based on triangle lattice

(b) Organic Motif based on Square Lattice

Figure 2.9: Pattern Examples

formed containers can be improved by different types of geometrical reliefs, their amount and arrangement. She also states that the important structural factors are the relationship between the width of the relief and its height. Furthermore, she proposes study of complex relief patterns and geometries on thermoformed surfaces by means of FDM moulds. These innovative and efficient designs can open up avenues personalisation and expression of brand identity. In another field study conducted by Rodriguez [98], thermoformed products with rib design variations were tested with consumers to perceive the influence of the final finish of the package and it was suggested that future reliefs should have more specific customization to achieve the desired differentiation on the packaging and strong consumer reaction.

2.3.2 Patterns

Pattern is ordered repetition of a unit. This recurrence of forms can be at regular intervals or increasing intervals. Nature is full of patterns from molecule lattices to wood grains, veins in a leaf to branches in a tree, petals of a flower to a snowflake. These universal forms when incorporated into man-made design can support and emphasise visual communication. As patterned forms repeat predictably, it creates balance, harmony and symmetry which help in defining relationship that can be interpreted intuitively and transfer information seamlessly. It is a key principles of design that when used effectively is aesthetically pleasing and optimizes the user experience [99].

The construction of every pattern, no matter how complex or simple the unit is based on a geometric plan. The skeleton of any pattern - geometric or organic is formed upon cross lines. These framework systems of cross lines, if there are two lines produce a square or diamond lattice depending on the angle, three cross lines will produce triangles and hexagons as seen in figure 2.9, [100].

Tessellations are type of patterns that like textures can be found in every culture. They can be found around the world in cultural artifacts, historical architecture and natural elements.

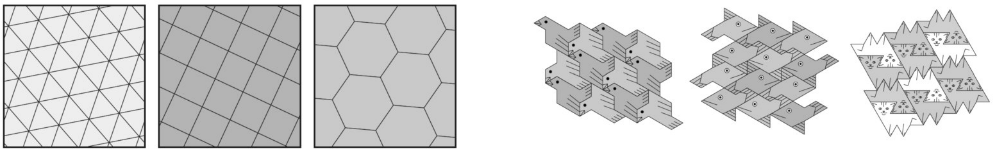

(a) Geometric Regular Tessellations **(b)** Simple Escheresque Tessellations

Figure 2.10: Examples of Tessellations

It can be defined as "Tesselation is a collection of shapes that fit together without gaps or overlap to cover the infinite mathematical plane. Another word for tessellation is tiling, and the individual shapes in a tessellation are referred to as tiles", [101].

Tessellations can be divided in to two groups:

- Geometric Tessellations - Tilings in which the individual tiles are geometric shapes are geometric tessellations.
- Escheresque tessellations - Tilings in which the individual tiles are real-world motifs are Escheresque tessellations. Where a tile is a set whose boundary is a single simple closed curve and generally possesses some sort of symmetry, mirror or rotational [101]. Few examples of tessellations can be seen in figure 2.10.

The next chapter discusses the application of the pin tool to thermoforming and the experiments that were conducted to explore the parameters of the pin tool that would maximise texture or details.

3 Experimental Work

In the following chapter, methodology, materials, configuration and tools used in the experimental setups is discussed. The experiments were conducted to determine an optimal set of parameters that would result in higher quality surfaces with maximum details in the reliefs. A preliminary set of experiments was also conducted to validate the prototype in the setup. Thus, the main experiments were divided into three parts:

- Experiment 0 To demonstrate the proof of concept of reconfigurable mould in thermoforming applications and to determine the capabilities and limitations of the prototypes in the thermoforming process.
- Experiment 1 To study the effect of process parameters.
- Experiment 2 To study the impact of design variables and determine their co-relation.

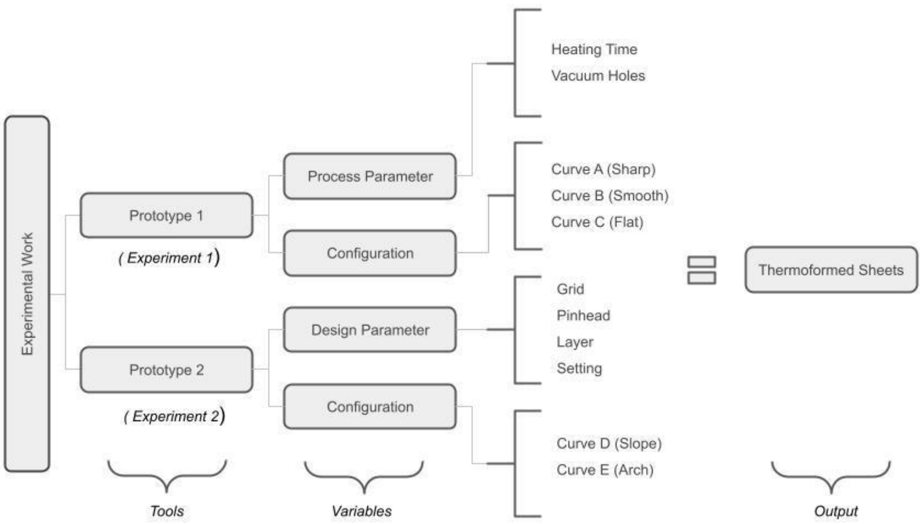

Figure 3.1: Overview of the Experimental Work

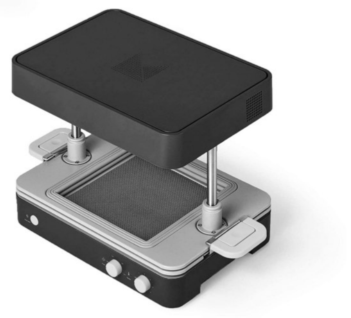

(a) Mayku Form Box

(b) HIPS Sheets

Figure 3.2: Experimental Setup

3.1 Equipment

Mayku FormBox is a desktop vacuum former as seen in figure 3.2 (a) and was used to carry out all the experiments. It was powered by a domestic vacuum cleaner and had a built-in heater with temperature range 160 - 340º C. The thermoplastic sheet was clamped on a silicon lined frame that slid on supportive guide rails from the heater to the bed. The forming bed was made of super fine steel mesh to increase airflow. The bed had the dimensions of 200 mm x 200 mm and allowed draw depth up to 130 mm. Time and temperature can be controlled with two dials located on the front of the machine. The Mayku FormBox can work with thermoplastic sheets such as PETg, HIPS, ABS, Polystyrene, Polypropylene, Poly-carbonate, Polyethylene and Acrylic PMMA with thickness range of 0.25 - 1.5 mm in thickness.

3.2 Material

High impact polystyrene (HIPS) sheet measuring 230 x 230 mm with 0.5 mm thickness was chosen due to its low cost and availability. It is one of the most widely used materials in this process as it an easy forming amorphous thermoplastic. It thermoforms with ease utilising low temperatures and fast cycle times. These are standard sheets that are available with Mayku Form Desktop thermoformer. The sheets are white in color, are able to replicate fine details and are ideal for prototyping and packaging as seen in figure 3.2 (b).

3.3 Experiment 0 and 1

The goals of the first set of experiments were the following:

- To test the prototype in the experimental setup.
- To determine the reproducibility of the experimental setup with surfaces that had different geometric sections.
- To explore and understand the influence of different process variables on the surfaces produced.
- To analyse characteristics of parts produced without the interpolation layer present.
- To propose modifications for the next prototype to be used in experiment 2.

3.3.1 Process Parameters

In this prototype no micro holes for vacuum were made, instead pins were removed, at the high and low points of the curve to record their influence. The sheets were heated to low and high values of 4 and 8 minutes respectively to register their response. The process parameters selected for this experiment were the following:

- Heating Time - 4 and 8 minutes
- Vacuum Holes - 2 and 6 holes

3.3.2 Tool

The pin-tool prototype used in the first set of experiments comprised of 372 pins, set in a matrix of 24 columns, each column containing 15 and 16 pins alternatively. The columns were misaligned to create a triangular packing arrangement that led a to denser matrix with high resolution [102]. The pins are spaced center to center 5.75 mm apart vertically and diagonally. For the purposes of testing the concept, steel construction nails, 70 mm in length and circular cross-section of diameter 3 mm, were used. The nails had a diamond shaped point and a wide hemispherical head of diameter 5 mm. As the nails were originally intended for rough work, tiny variations were found from pin to pin in size and shape. The prototype is depicted in figure 3.3.

The pins were held in two aluminium plates (6 mm thickness each) with a rubber sheet (3 mm thickness) between them. The holes in the rubber layer had a smaller cross-section

Figure 3.3: Prototype for Experiment 1

that created friction and held the pins in desired position. Layers were clamped together with hexagonal bolts that locked the pins in position by applying lateral compressive loads [24] and could be loosened to release tension in the rubber layer and making it easier to reset the tool. The stand is made of female dowel pins made of aluminium. After the first set of exploratory experiments, a makeshift skirt of duct-tape was added to seal the mould. The maximum pin height that could be drawn with this prototype is 40 mm.

3.3.3 Configuration

In the first experiment process parameters were varied to evaluate the transmission of the details from the nail heads to the sheet formed. Experiments were conducted without the interpolator layer with the main intentions of exploring the effect of the pin tool on the surface quality on different shapes.

The pin-tool was actuated into three distinct single curves as seen in table 3.1. The surface A had a 45 degree positive and negative incline with a sharp peak and valley. The surface B had smooth concave and convex sections. The surface C had flat and a sharp 90º degree step. All three surfaces were chosen to create a baseline of different geometric shapes that can be formed using the moulds. A, B and C all had same area under the curve and the same amplitude.

3.3.4 Process

The pin tool was actuated manually, for this purpose three master models were 3D printed. These templates were first modelled in SOLIDWORKS®. The curves A, B and C were sketched, offsetted and extruded to fit the prototype dimensions. The STL file was exported to a FDM printed, Flashforge - Creator 3, and printed in PLA material. The templates were then attached over the bed as seen in figure 3.4. The pins were then pushed one by one until the head hit the underside of the template.

After loading the configuration into the pin tool the sheets were thermoformed following the process as shown in figure 3.5. Each experiment as seen in table 3.1 was repeated thrice

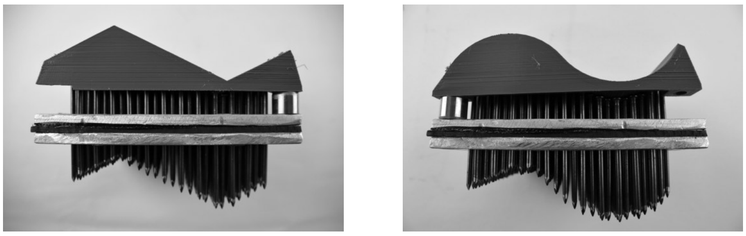

(a) Template for curve A **(b)** Template for curve B

Figure 3.4: 3D Templates Modelled in SOLIDWORKS®

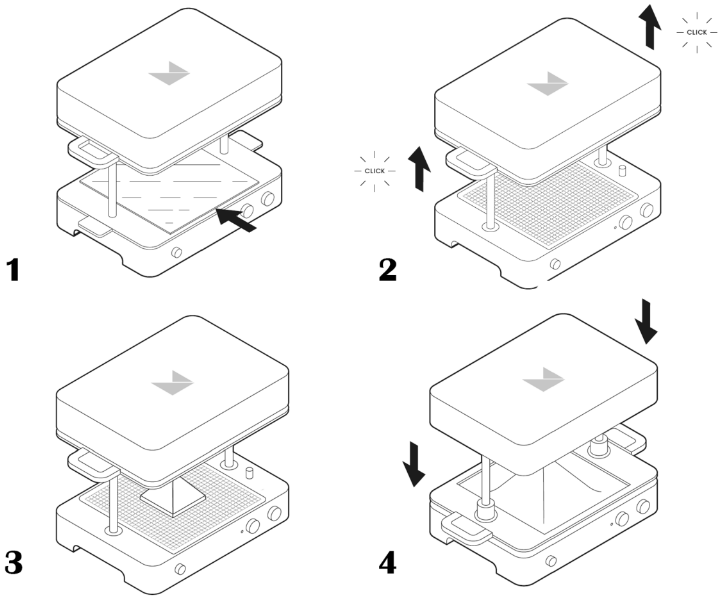

Figure 3.5: Experiment Process - (1) Preheat the heater to the required temperature setting. Prepare and load the sheet into the tray (2) Clamp it into the top half of the tray near the heater. (3) When the sheets shows ripples place the mould on the bed (4) Press the frame with the sheet on the mould, wait for it to cool for 10-20 seconds then trim and demould.

Table 3.1: Process Parameters where A (Sharp), B (Smooth), C (Flat) are single curves

Curvature	Heating Time	Vacuum Holes	Name
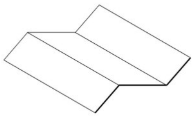	4min	6	A1
	8min	6	A2
	4min	2	A3
	8min	2	A4
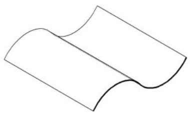	8min	2	B1
	4min	2	B2
	4min	6	B3
	8min	6	B4
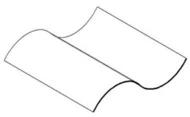	4min	6	C1
	8min	6	C2
	4min	2	C3
	8min	2	C4

for reproducibility.

3.3.5 Evaluation Method

Each surface was evaluated by the following method. Each pin was categorised according to its definition, if the outline of the head is clearly distinct then the pin is assigned full definition (f) status. If the pin is visible but parts are missing or not sharp, it is assigned medium definition (m) status. If the pin is barely visible or missing it is allocated as low definition (b). All three status F, M, B were assigned numeric value of 2, 1 and 0 respectively. Each column was then calculated to find its aggregated amount. Then it is compared with expected value of the column if it was fully defined. Example can be seen in appendix A.

3.4 Experiment 2

The goal of the experiment second set of experiments were to determine the following:

- To test the prototype in the experimental setup.
- To determine the reproducibility of the experimental setup with surfaces that had different inclines and number of pins.
- To determine the best set of design parameters.

3.4.1 Design Parameters

Design of experiments (DOE) is a statistical analysis tool that enables study of the relationship between multiple input factors and key output variables. It allows multiple input factors to be manipulated, determining their effect on a desired output. By evaluating the response of multiple inputs on an output variable at the same time, DOE can identify important interactions that may be missed when experimenting with one factor at a time. All possible combinations can be investigated (full factorial) or only a portion of the possible combinations (fractional factorial).

This analysis was carried out by reproducing a partial factorial model. In each experiment depending on the DOE and the configuration, the pin tools was assembled differently. The variables were divided into four categories with two values each with a total of 16 experiments to be conducted but with DOE fractional factorial of 8 experiments with one replication for reproducibility.

The four design parameters that were used to configure the prototype are explained below and can be seen in table 3.2.

Table 3.2: Design Parameters

Design Parameters	Value 1	Value 2
Grid	Triangle	Square
Layer	With	Without
Pinhead	Square	Hexagon
Setting	Positive	Negative

Grid The usage of grids for pin arrangement allowed for uniform pin packing. Grids are built from repetition of simple regular polygons. Two different layouts were compared, square and triangle. Square grids are the most common type of grid in 2D applications as they are simpler and easier to map. In triangular grids, pin density is higher, increasing the resolution. Pins in both grids were located at each vertex of the grid.

Layer In pin based tooling an interpolation layer is usually used to provide a smooth surface to form the plastic as well as to prevent waviness formed by the pins. As our purpose is to maximise details interpolation layer is omitted from this experiment. Instead, the notion of interlayer is introduced, which is a perforated layer that would be placed below the pinheads. This would theoretically stop the draw of the thermoplastic while still allowing the reproduction of details.

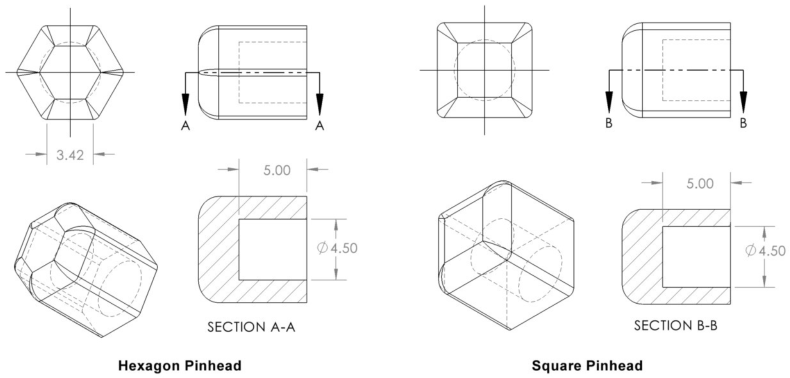

Figure 3.6: Sheet drawing of Pinheads

Setting Positive and Negative tooling is an important factor in thermoforming. In positive tooling, also knows as male moulds the shape protrudes up and the formed plastic at the top of the mould is thickest. Generally, it is employed when a less precise, more rounded shape is required without sharp angles, or intricate surface details. In negative tooling, or female moulds, the shape resides inside the cavity. As it pulls the plastic inside the tool more crisp parts can be formed. When the plastic cools it shrinks away from the female mould which allows easier demoulding. However, a male mould needs the use of draft angles to allow for removal. In both cases, thickness distribution also varies greatly. Reconfigurable pin moulds are typical male type tooling, as the sheet always forms onto the mold. But the same curve can be reproduced in positive or negative image. The third parameter is finding which curve setting would be better for detail reproduction. [103].

Pinhead Square and hexagon prismatic shape were modelled in SOLIDWORKS® as seen in figure 3.6. 160 pieces of each were 3D printed using Flashforge - Creator 3, FDM Printer in PLA material. These are form the details that were translated in the plastic pats. The pins were 8 mm in height and 6 mm in width with rounded corners.

3.4.2 Tool and Configuration

The pins were formed with zinc plated threaded steel rods with 4 mm diameter that was cut in 60 mm length each. These were then placed in two different beds made of 14 x 14 mm plywood with 5 mm thickness. The pins were arranged in two formats, grid with triangular layout and grid with square layout that had 169 and 164 pins respectively. The pins were locked in their position with bolts and washer.

The second set of experiments were done to figure out the best design parameters in a three dimensional surface for detail reproduction. The experiment was designed using the

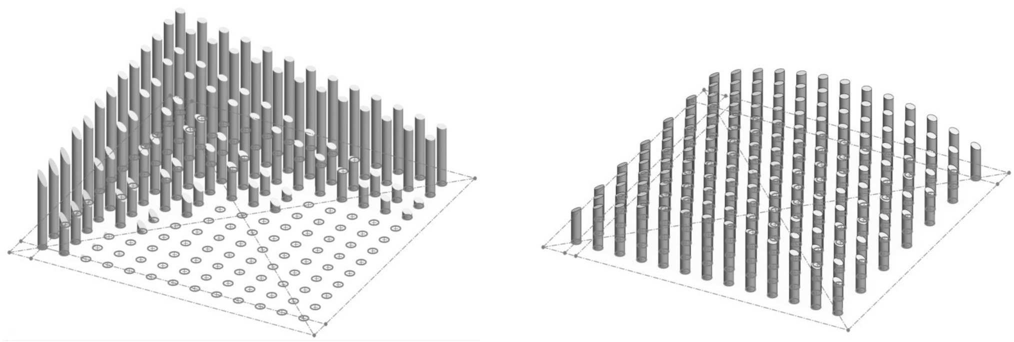

(a) Curve D in Square Grid **(b)** Curve E in Triangle Grid

Figure 3.7: Modelling in SOLIDWORKS®

program Minitab® Statistical Software Version 20.2 as seen in table 3.3

The configurations were repeated for this purpose in two surfaces, curve D & E. The curve D is made of inclines ranging from 10-60% and curve is an arch of 140 mm radius. The fractional factorial design experiment was repeated for both the curves. Thus, the experiment was divided into two parts (a) & (b).

Table 3.3: Fractional Factorial DOE for Experiment 2

Configuration	Grid	Pinhead	Layer	Setting
SSNP	Square	Square	No	Positive
SSYN	Square	Square	Yes	Negative
TSNN	Triangle	Square	No	Negative
SHYP	Square	Hexagon	Yes	Positive
SHNN	Square	Hexagon	No	Negative
THYN	Triangle	Hexagon	Yes	Negative
TSYP	Triangle	Square	Yes	Positive
THNP	Triangle	Hexagon	No	Positive

3.4.3 Process

From the configuration, both the curves were modelled in SOLIDWORKS® and the pin were manually positioned according to the layout as seen in figures 3.7. These pins were then set according to these measurements and locked into place with a bolt & washer on both side of the bed. Subsequently, the layer and the pinheads were placed. The assembled tools can be seen in figure 3.8.

The thermoforming process followed was same as described in the figure 3.5.

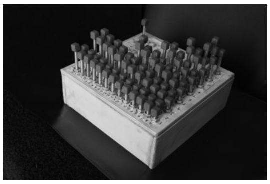

(a) Isometric View

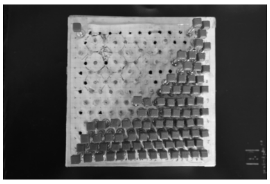

(b) Top View

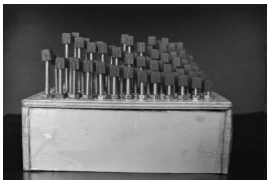

(c) Side View

(d) Isometric View

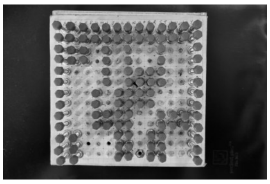

(e) Top View

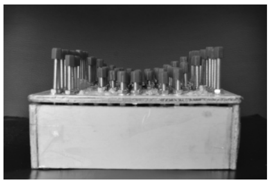

(f) Side View

Figure 3.8: Prototype Example for Experiment 2, (a)(b)(c) Curve D with configuration TSNN & (d)(e)(f) Curve E with configuration SHNN

	A	B	C	D	E	F	G	H	I	J	K	L	M
10	o	o	o	o	o	o	o	o	o	o	o	o	o
	o	o	o	o	o	o	o	o	o	o	o	o	o
20	o	o	o	o	o	o	o	o	o	o	o	o	
	o	o	o	o	o	o	o	o	o	o	o	o	
30	o	o	o	o	o	o	o						
	o	o	o	o	o	o	o						
40	o	o	o	o	o								
	o	o	o	o	o								
50	o	o	o										
	o	o	o										
60	o	o											
	o	o											

Curve D (Slope)

	A	B	C	D	E	F	G	H	I	J	K	L	M	
0	o	o	o	o	o	o	o	o	o	o	o	o	o	0
	o	o	o	o	o	o	o	o	o	o	o	o	o	
1	o	o	o		o		o			o			o	6
	o	o	o		o		o			o			o	
2	o				o		o	o	o	o			o	7
	o				o		o	o	o	o			o	
3	o			o		o	o	o	o				o	8
	o			o		o	o	o	o				o	
4	o			o	o	o	o			o	o	o	o	9
	o			o	o	o	o			o	o	o	o	
5	o	o				o	o		o	o			o	10
	o	o				o	o		o	o			o	

Curve E (Arch)

Figure 3.9: Depiction of pin arrangement in different sections of Curve D (Left) & E (Right)

3.4.4 Evaluation Method

The curve D is divided into six sections of two rows each. The first section had 10º slope with the starting pin having 40 mm actuated height. Similarly for the other five sections with 20º , 30º, 40º, 50º, 60º slope respectively. This configuration was calibrated to define at which angle the details start getting lost.

In curve E, the arch is divided into ten sections. Each made up of two rows as seen in figure 3.9. Section 1 to 5 from column A to G and section 6 from column G to M. The first two rows had all the pins forming the curve while the sections had pins removed at random intervals. This was done to determine the number of pins required to reproduce a curve while getting the highest definition.

The surface evaluation was performed considering two factors, the first one as in the previous exercise, quantifying the amount of pinhead edges registered on the thermoformed sheets. Higher value was assigned to those pins with more edges visible on the surface of the sheet. The second factor is the depth of the depressions formed due to space between the pins of each of the curves was evaluated. The depressions were measured by quantifying the distance between a static horizontal reference plane and the curve points in the x and y coordinates. Section 0 was considered the reference for the depression values and the values furthest from it were penalized to a greater extent. These two values were averaged and a unique value was assigned to each of the curves. This value allowed to evaluate the impact and co-relation of each of the four design variables by applying a DOE analysis.

4 Results and Discussion

In this chapter, the results of the two experiments according to the evaluation method are presented. The relationship between different process and design variables was defined and their effect on the definition of details in the thermoformed surfaces was evaluated. Set of geometric sections that produce superior features as well as minimum and maximum arc length ratios between continuous pins were defined. In addition, set of four-factor configurations that showed better resolution of the formed surfaces were obtained. Results are discussed according to the particular order they were done.

For the purpose of this work the surface quality is defined according to the number of pinhead edges registered on the thermoformed sheet. Higher the definition, more detail would be registered.

4.1 Results of Experiment 0

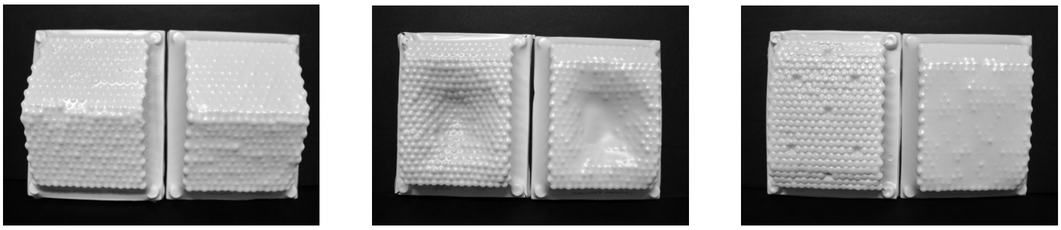

(a) Inclined surface, with (left) and without vacuum holes(right)

(b) Parabolic Surface, with (left) and without vacuum (right)

(c) Shallow surface, with (right) and without interpolator layer (left)

Figure 4.1: Formed sheets from Experiment 0

Qualitative analysis from the experiment 0 led to these observations:

- After manufacturing the prototype, the resolution is set and this can become a limitation if details required are smaller than the cross section of the pins. As can be seen in the figure 4.1a where the peak is the same width as the head of the pin. However, bigger cross sections can be obtained by combining pins with a common pinhead.
- Changing the shapes of the pin tips, increasing their cross-sectional area and variation in their spacing or missing pins can lead to different patterns. These aspects of the pin tips can create different tiling as seen in figure 4.1c

- Without the interpolator layer, part removal from the mould is very difficult and can even lead to damage. This is mainly due their being no draft angle on the pin shank and undercuts on the pinhead as seen in figure 4.1c. Ejector pins that are connected with a band that prevents undercut could help in demoulding.

- The two sides of the reconfigurable mould create negative and positive of the surface to be formed which creates two different types of details embossed and engraved.

- Vent holes for the vacuum need to be distributed uniformly in the bed especially for deeper draws and details as seen in 4.1b. This would benefit in forming different curves that have changing geometric sections.

- Orientation and movement of even a single pin can register as error and can be hard to control when working with high resolution moulds.

- Another limitation of the mold is the length of the pin. The part of the pin that is not actuated remains below the bed and draw depth space in the setup.

From this experiment, it was concluded that curves with different geometric sections could have different definition levels using the same parameters. Thus, the next experiment would examine the formed surface definition for different cross sections wile varying process variables like vacuum holes and heating time.

4.2 Results of Experiment 1

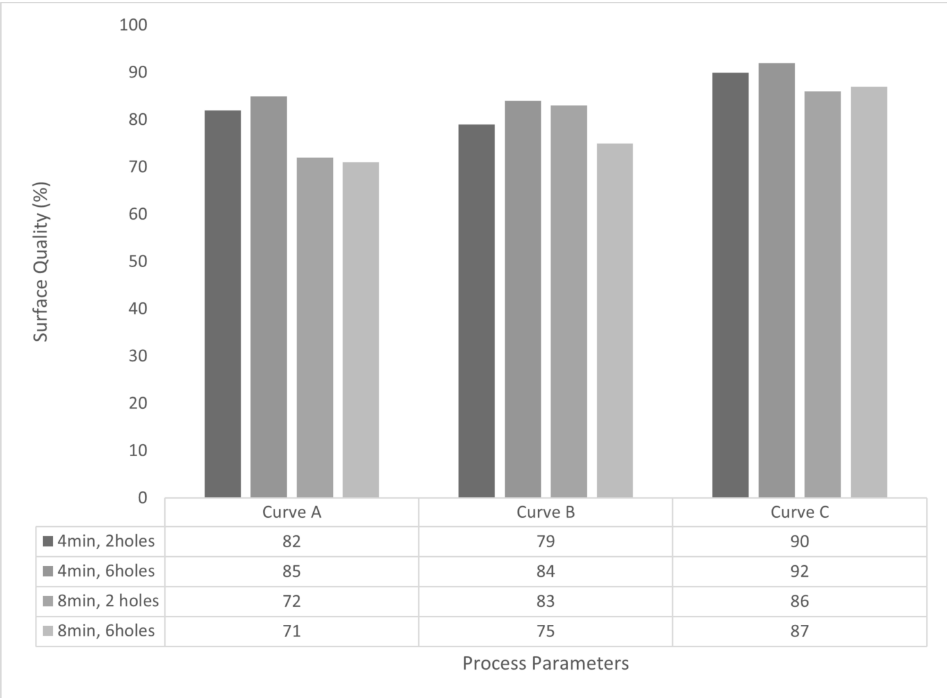

	Curve A	Curve B	Curve C
4min, 2holes	82	79	90
4min, 6holes	85	84	92
8min, 2 holes	72	83	86
8min, 6holes	71	75	87

Figure 4.2: Result of Experiment 1, Process Parameters (Heating Time and Vacuum Holes)

The experiment was conducted with the same tool used in experiment 0. The sheets samples that exhibited, the best surface quality are pictured in figure 4.3 and 4.4. As seen in the figure 4.2, analysis of all the surfaces formed, showed that the best surface quality is exhibited by curve C overall, whereas the least surface quality is exhibited by lowest sections of curve A and B. This can be attributed to the flat horizontal sections of curve C where all the pinheads are perpendicular to the plastic sheet at the time of forming resulting in an even contact with the pins. Meanwhile in both curves A and B, the sheet touches tangentially with the pinhead edges with less contact points as seen in figure 4.6. Curve A and B have similar number of tangential contact points. Example of matrix weighted evaluation of curve A is shown in Appendix A.

Curves that were formed at 4 minutes performed the best in their curve type. There was a slight increase in definition in curves that that time when formed with 6 vacuum holes. However, it should be noted that, the variance in heating time had more direct effect on the performance compared to the quantity of vacuum holes. The reason for this could be that once the sheet reaches the forming temperature it sags. This increases the distance between the sheet and the heater and the sheets starts to cool down and is at a lower temperature when formed.

(a) Curve A - Incline sections with peak and valley (t= 4 min; 6 vacuum holes)

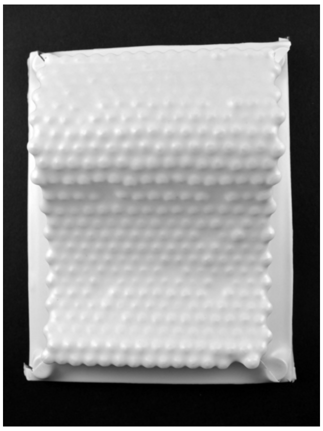

(b) Curve B - Convex and Concave sections (t= 4 min; 6 vacuum holes)

(c) Curve C - Horizontal and Vertical Sections (t= 4 min; 6 vacuum holes)

Figure 4.3: Top View of Formed Sheet from Experiments 1

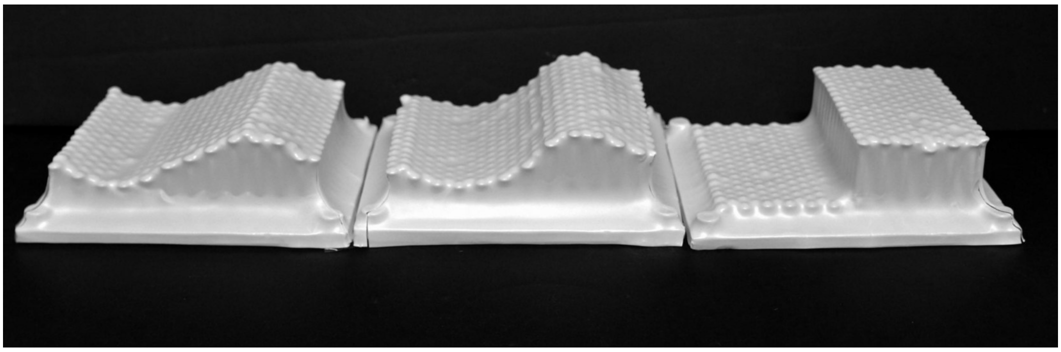

Figure 4.4: Side View of Formed Sheets From Experiment 1, Curve A, B and C

Column	1	2	3	4	5	6	7	8	9	10	11	12	13	14	15	16	17	18	19	20	21	22	23	24
							Peak											Valley						
	(a) ←					→										(b) ←					→			
A	95%	84%	79%	87%	83%	84%	100%	100%	100%	100%	100%	95%	100%	100%	100%	92%	86%	29%	32%	65%	78%	97%	103%	100%
						Highest Point										Lowest Point								
	(c) ←					→					(d) ←							→						
B	97%	78%	75%	76%	86%	84%	100%	97%	97%	97%	83%	91%	90%	85%	87%	56%	56%	78%	93%	95%	95%	56%	100%	95%
													Step											
													(e) ←	→										(f) ↔
C	100%	100%	95%	100%	100%	95%	100%	100%	100%	100%	100%	100%	20%	46%	100%	100%	100%	100%	100%	100%	100%	100%	100%	85%

Figure 4.5: Comparison of different sections of Curves A (Sharp), B (Smooth) & C (Step)

Comparisons of different section heights and shape in curve A, B and C showcased that sheet-to-mould contact point is a also factor for better renderings. The next group of observation have been made respect to the figure 4.5

- Curve A at it peak column had the best definition at 100% while the valleys were the worst defined with average value of 6.5%. As the peak is the first touch point for the thermoplastic sheet.
- The section (a) and (c) were inclined sections leading to the peak. They exhibited less amount of detail compared to their directly opposite counterpart. A possible explanation could be the placement of all the vacuum holes on the opposite side of these sections or could be attributed to wall thickness.
- The worst rendering in the entire curve is in the section (b) which was the sharp valley with the lowest pin placed in column 18. As the pins go up to the mouth of the valley the amount of details increases. It should be noted that these results are despite the placement of vacuum holes in the column. One reason for this is the sharp tapering of the valley into a pointed edge. Comparatively, same points in curve B are rendered intensely due the curve being smoother and definition of 78%, compared to 29% of curve A. Thus it is surmised that, valleys with larger radii will perform better.
- In curve B, highest and lowest points were located in columns 6,7,8 and 17,18,19 respectively with 93% and 72% performance. The section (d) starts from high definition and fades into low definition. This is because this convex slope section becomes progressively steeper downhill leading to bad definition. The plastic stretches from the sheet that is not contacting the mold surface, thus the plastic stretches into the bottom section last.
- In Curve C, Section (e) has the worst definition in all the three curves as the entire column 13 is missing because of the sharp 90º degree angle in the step. The column next to it is also affected before the curve flattens horizontally. This phenomena is investigated further in the next experiment. The section (f) is actuated close to the surface of the pin bed placing them closer to the protruding dowels pins in the corner. Thus, the placement impacted the quality of the pins in the corner.
- Lastly all the border edges have higher rendering at A 91%, B 94% and C1 92% as seen in figure 4.4

4.2.1 Findings of Experiment 1

It is concluded that formed sheets with 8 min of heating time present less definition than their similar with 4 min. One of the reasons for this result might be the drop of the sheet temperature below its ideal forming temperature. Thus, the temperature where the sheet starts to sag which is a manifestation of the lowering tensile strength will output better definition. Equivalent details in the whole surface is desired, otherwise, sections with lower level of details can present as defects. For this, the pin configurable mould should have vacuum holes distributed throughout the mold, especially surrounding each pin.

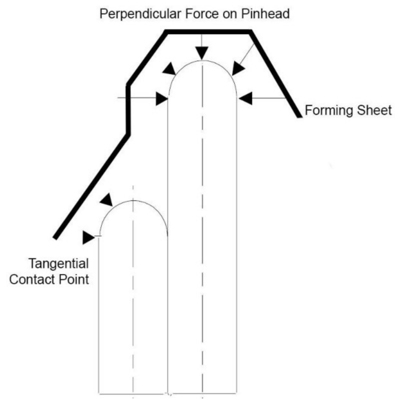

Figure 4.6: Contact Points

The pressure force applied by the forming press on the pin bed is evenly distributed to all contact points. Starting from the highest points and descending to the base. The contact points of each pin are a function of the relationship of height and horizontal distance to those surrounding it. The contact points of the pin head and the details marked on the thermoformed sheet are proportional.

Thus in the next experiment the prototype will have vacuum hole distributed throughout the mold and will be used to test the effect of different inclines as well as of relationship between two pins on the reproduction of details is inspected.

4.3 Result of Experiment 2

The effect of four process variables on the etching of details on thermoformed surfaces was evaluated by means of a DOE analysis. A new set of tools with two different spatial configurations was used for this experiment. The incidence of the process variables was evaluated by quantifying the number of etched corners and the amount of waving present in the formed part. A range of arc lengths between continuous pins has been defined, combining an ideal mathematical model in conjunction with experimental results.

The section is divided into two part the first analyses is of the curve D (slope) as seen in figure 4.7 & 4.8 and the second analyses is of curve E (arch) as seen in figure 4.9 & 4.10. Example of matrix weighted evaluation of curve D and E are shown in Appendix C.

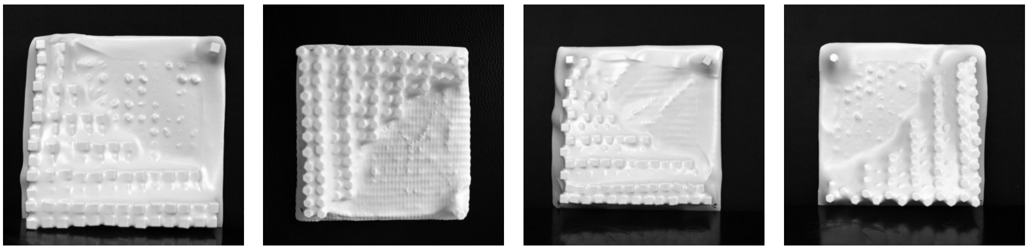

(a) SSNP **(b)** SHYP **(c)** TSYP **(d)** THNP

Figure 4.7: Experiment 2(b) Results Curve D (Slope) - Positive Setting

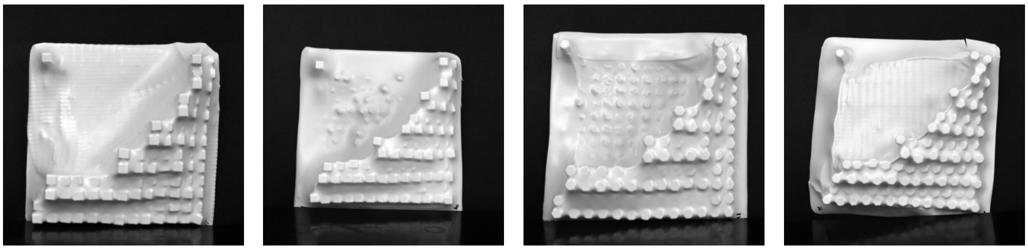

(a) SSYN **(b)** TSNN **(c)** SHNN **(d)** THYN

Figure 4.8: Experiment 2(b) Results Curve D (Slope) - Negative Setting

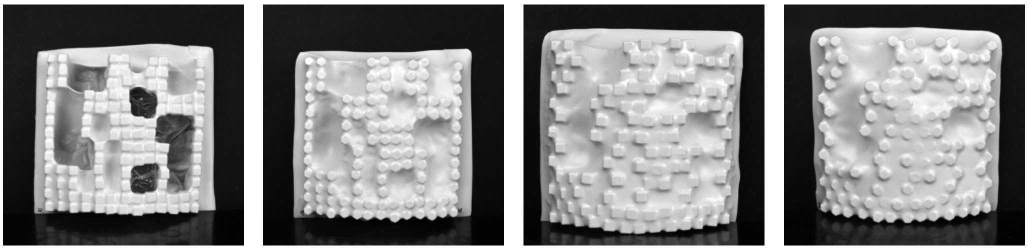

(a) SSNP **(b)** SHYP **(c)** TSYP **(d)** THNP

Figure 4.9: Experiment 2(b) Results Curve E (Arch) - Positive Setting

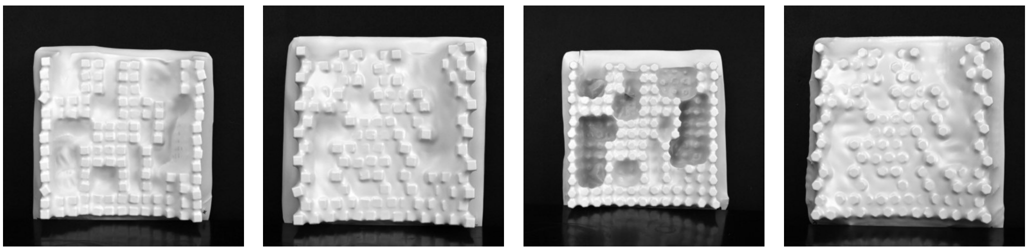

(a) SSYN **(b)** TSNN **(c)** SHNN **(d)** THYN

Figure 4.10: Experiment 2(b) Results Curve E (Arch) - Negative Setting

4.3.1 Results of Experiment 2(a)

4.3.2 Experiment 2 (b)

The curve slope in each configuration was divided in six sections, with increment of 10 degrees, going from 10% incline to 60% incline. As indicated in the figure 4.11 the highest definition is obtained in 10% incline and the lowest definition in 60% incline in all configurations. This result is because at a given pin resolution, with all pins actuated, slope with less % incline has not only more pins forming the curve but also more contact points touching directly on each pin as seen in figure 4.12.

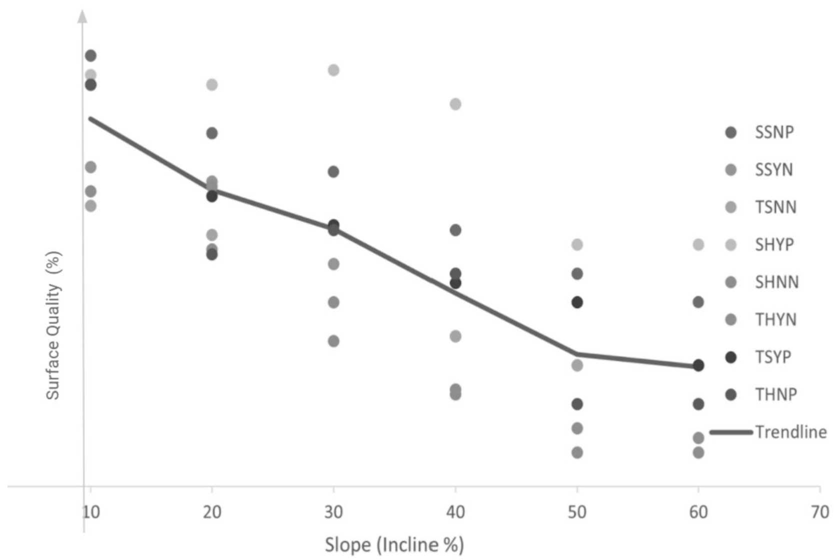

Figure 4.11: Result of different inclines in each configuration

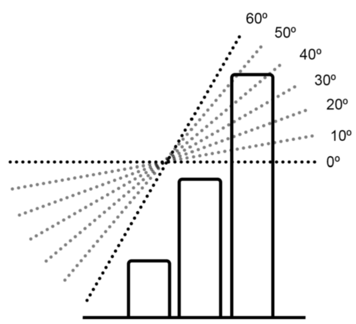

Figure 4.12: Direct Contact points with the Pin

Out of the four factors, setting had the greatest impact on the thermoforming process of plastic sheets as show figure 4.13. The configurations in which positive settings was used had significantly more definition than curves in negative setting. In this setting, most pins are in higher positions in Y axis, which causes an improvement in the quality of the engraved

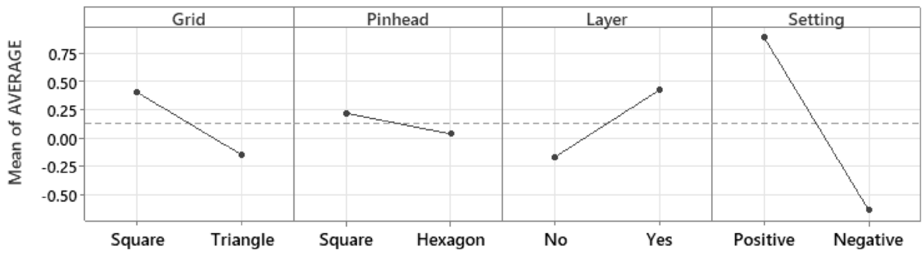

Figure 4.13: DOE Mean Plot of Curve D

details in the thermoformed sheet. In the specific case of this test, this can be explained by the spatial location of the pins and the ventilation holes for air suction inside the part during the thermoforming process. DOE mean plots of each incline can be referred to in Appendix B.

The reasoning being, in the positive setting, the free space in the pins is adjacent to the lower values of the pin height. The air gets suctioned from the highest to the lowest point, creating a greater vacuum. This is the opposite of what happens in the negative setting where the free space of pins is located at the back of the highest pin height values. In this scenario the air generates a suction effect between the highest point and the back of the mold, creating a loss of detail in the front pins of the curve.

The type of grid and the presence of layer presents are the next two important factors. The grid with square configuration is the one that generates a greater detail in the thermoformed sheet for inclinations above 10%, it is explained by the space between pins that avoids the overlapping. The presence of the mesh interlayer used below pins had a positive effect as it helped in stopping the draw of the sheet in sections where pins were not actuated.

The pinheads do not present a significant effect in the definition of thermoformed sheets, however it is evidenced that for inclinations higher than 20% the number of edges that can be replicated decreases, in this experiment there were 6 and 4 edges of hexagon and square pinheads respectively. However, it should be noted that if the number of edges is increased to the point of generating a circumference, this appreciation changes as it is considered as a single point of contact.

For the Experiment 2(a) data, two cubes display all combinations of 4 thermoforming factors settings evaluated and the fitted mean for each combination. The cube on the left shows the response means when positive setting is used. The cube on the right shows the response means when negative setting is used. Cube plot is used to predict the fitted means at all the factorials in the design.

The second best combination is the one that was carried out in the laboratory with a mean value equal to 2.10475, located in the higher left back corner of positive setting cube as showed in the figure 4.14. This is SHYP configuration - positive setting, in a square grid with layer present and hexagon pinheads.

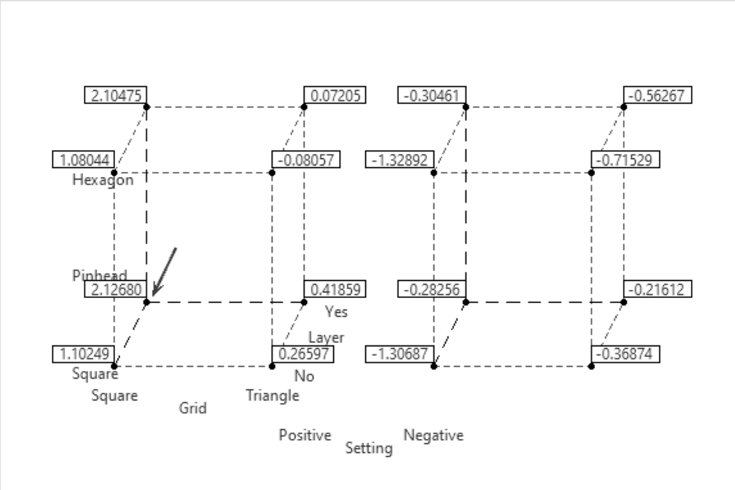

Figure 4.14: DOE Cube Plot of Curve D

According to the cube plot surface slope figure 4.14, the combination that presents the highest fitted mean is the one with the code SSYP a mean value equal to 2.12680, point indicated by the red arrow. This was not carried out within the group tested due to the factorial partitioning but was extrapolated by means of the DOE statistical analysis. The combinations of factor - positive setting, in a square grid with layer present and square pinheads, is considered to be the best among the all possible factorial combination. Both values agree considering that the only difference is that of the pinhead.

The Arch slope was divided in 10 sections plus section 0 used as reference. The reference section had all pin positions filled, in the other sections, two or more pins were randomly removed in order to evaluate the incidence of the spatial positioning of the pins along the pin bed on the detail definition and the stability of the thermoformed sheet. Out of the 10 sections analyzed in this experiment, section 1 as seen in table 4.1 with gaps at column D and F of the grid, had best details in the thermoformed sheet, even above the curve used as a reference which contained pins at all positions. This is because, as the reference curve in section 0 approaches its highest point, the height differences between the pins become narrower, resulting in a loss of detail caused by overlapping and draft in the curve also known as the staircase effect. Removing the pins from the D and F position eliminates this problem.

Section 1 with an average equal to 2.0 is the one that presents the highest value in relation to the other sections, considering all the configurations tested in the laboratory. For section 1 the best performing configuration was the one with the code SHYP. This configuration is consistent with the highest coefficient within the cube plot of DOE arch.

Table 4.1: Result of Experiment 2 (b)

	Section									
Configuration	1	2	3	4	5	6	7	8	9	10
SSNP	1.95	0.27	0.34	0.32	0.23	0.55	0.34	0.30	0.52	0.37
SSYN	2.36	0.23	0.29	0.64	0.26	0.38	0.48	0.33	0.68	0.88
TSNN	0.67	0.17	0.22	0.25	0.24	0.19	0.28	0.24	0.50	0.24
SHYP	3.50	1.91	1.46	1.20	1.27	1.79	2.31	1.48	2.39	1.75
SHNN	0.81	0.34	0.34	0.29	0.11	0.09	0.21	0.14	0.13	0.25
THYN	1.87	0.76	1.17	0.91	0.22	0.96	0.79	0.48	1.46	1.28
TSYP	2.36	0.23	0.29	0.64	0.26	0.38	0.48	0.33	0.68	0.88
THNP	2.49	0.53	0.78	0.74	0.29	2.43	1.63	1.38	1.68	3.38
Average	2.00	0.55	0.61	0.62	0.36	0.85	0.82	0.59	1.01	1.13

From the DOE mean plot of the four factors as seen in figure 4.15 it can be observed that the factor that has the highest effect in the reproduction of details along the thermoformed sheet is the grid and setting, at the response value of square layout and positive setting. This is explained by the spatial location of the pins along the grid, in the square grid the pins have crisper edges as there are no intermediate pins at the same time the missing sections have limited span and are also in alignment.

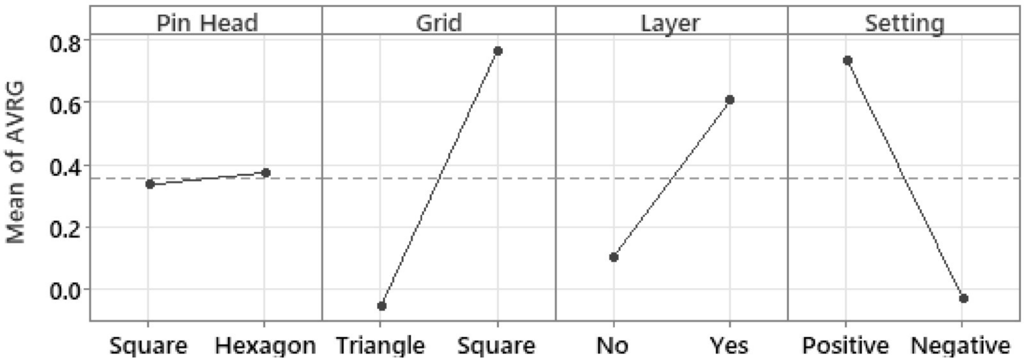

Figure 4.15: DOE Mean Plot of Curve E (Arch)

The positive mold allows more details of the arc-shaped curve to be captured as shown in the DOE average graph. This can be explained by the trajectory that the sheet follows when it is thermoformed. In which the highest points are those that first come into contact with the sheet, giving the best definition at those places.

At lower points there is usually also a reduction in the thickness of the sheet as it stretches, sometimes resulting in critical failure. The use of the mesh between pins serves as a support material for the structure in cases where the distance between pins generates slopes close to 90 degrees. It is mainly important in the configuration using positive setting molds, due to the height gradients between missing pins.

Two cubes display all combinations of 4 thermoforming factors settings evaluated and the fitted mean for each combination into the experiment 2(b). The cube on the left shows the response means when positive setting is used. The cube on the right shows the response means when negative setting is used. Cube plot is used to predict the fitted means at all the factorials in the design, and present the combination SHYP as the one with the highest fitted mean. Point marked with a red arrow in the figure 4.16 and with a value equal to 1.69001. The combinations of factor - positive setting, in a square grid with layer present and hexagon pinheads, is considered to be the best among all the possible factorial combination.

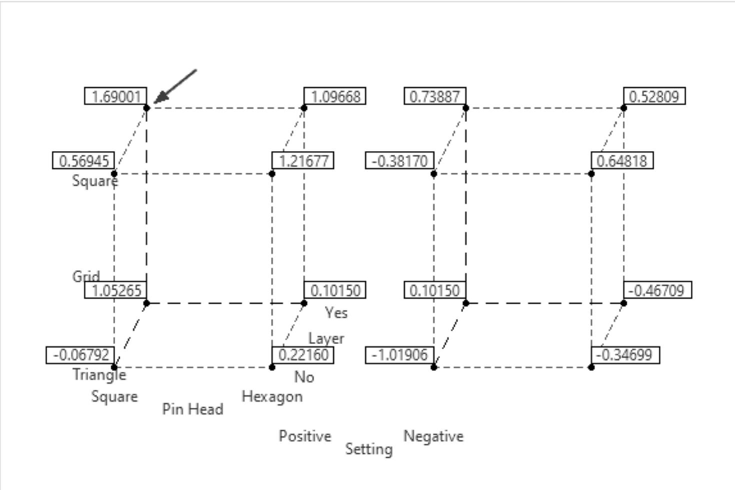

Figure 4.16: DOE Cube Plot of Curve E (Arch)

If it is analyzed that the incidence of the pin head is minimal with respect to the other factors as shown in figure 4.15, a concordance and relationship with the results obtained in test 2(a) is determined.

4.3.3 Calculation of Height and Distance Ratio

Based on the data obtained from experiment 2, it is proposed to define the minimum theoretical distance between two adjacent pins that have different heights. This minimum distance as shown in figure 4.17b is required for all the details of the pinhead to render in the formed sheet. In addition the maximum distance is also obtained between the same pins in order not to compromise the stability of the structure due to sagging in the formed sheet as seen in figure 4.17c.

It can be ideally expressed that the curve to be drawn between two pins with different heights, at a distance x as shown in figure 4.18is that of a rectangular hyperbole. The general equation of a rectangular hyperbole is presented in the equation 4.1

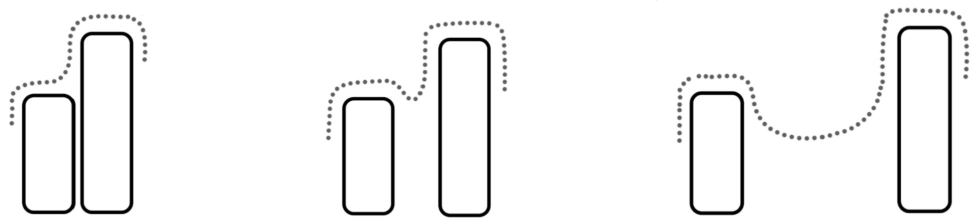

(a) Pins that are too close lead to overlapped details

(b) Pins at a model distance with defined edges

(c) Pin that are too far have defined edges but with formation of a sag

Figure 4.17: Distance between two adjacent pins

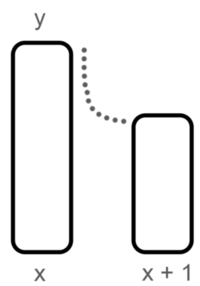

Figure 4.18: Arc Length Diagram

$$(x-h)(y-k) = m \tag{4.1}$$

Where m represents a constant and h and k are the coordinates of the center of the hyperbole. The arc length of the curve is determined by considering the maximum height of the designed pinheads which is 8 mm. This value is assigned as the constant m.

The curve of the figure 4.19 has as its origin coordinates the point (0,0). The vertex of the curve is at the coordinates indicated in equation 4.2.

$$v = (h+\sqrt{2m}),(k+\sqrt{2m}) = (\sqrt{\frac{8}{5}}),(\sqrt{\frac{8}{5}}) \tag{4.2}$$

The arc length of a curve is defined according to the following equation 4.3:

$$\mathrm{d}s = \sqrt{(\mathrm{d}x)^2 + (\mathrm{d}y^2)} \tag{4.3}$$

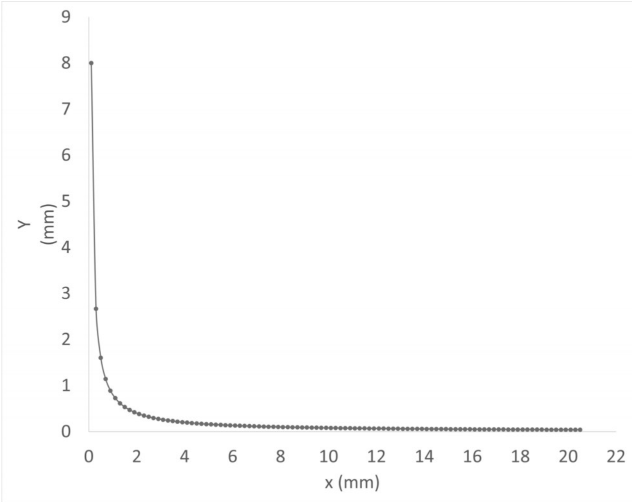

Figure 4.19: Hyperbole $y = \frac{0.8}{x}$

$$s = \int \sqrt{(\mathrm{d}x)^2 + (\mathrm{d}y)^2} \tag{4.4}$$

For $f(x) = \frac{0.8}{x}$

$$x = \frac{4}{5}\frac{1}{y}\mathrm{d}x = \left(\frac{4}{5}\right)\left(\frac{-1}{y}\right)\mathrm{d}y \tag{4.5}$$

The integration will be given as a function of the ordinate variable. Replacing in 4.4 results in:

$$s = \int \sqrt{(\frac{4}{5})(\frac{-1}{y})\mathrm{d}y)^2 + \mathrm{d}y^2} = \int \sqrt{(\frac{16}{25})(\frac{1}{y^2}) + 1} + \mathrm{d}y \tag{4.6}$$

For the limits it has been considered to divide the integral in two parts, the first one from the highest point of the curve that represents the final position of the pin number one to the vertex of the hyperbolic curve. And the second segment is considered from the vertex to the right until reaching the initial position of the new pin. For the calculation of the integral the program Maxima Open Source Computer Alegra System 5.45.1 was used. Using the commands shown in 4.7 and 4.8 the first portion of the curve of the depicted in figure 4.19 is integrated.

$$quad_q ag(sqrt(1 + (16/25) * (1/y^2)), y, sqrt(8/5), 8, 1); \tag{4.7}$$

$$quad_q ag(sqrt(1 + (16/25) * (1/y^2)), y, 0.1, sqrt(8/5), 1); \tag{4.8}$$

Where the first value of the line (%1) represents the integral of the curve that in this case is equal to 6.94 mm, which represents the length of the arc from the end point of the pinhead at position x with height of 8 mm. The second part of the integral from the vertex of the hyperbole to the starting point of the new pinhead was defined at 2.43 mm consider the remaining distance to complete the curve.

```
Maxima Open Source Computer Algebra System 5.45.1
Maxima 5.45.1 https://maxima.sourceforge.io
using Lisp SBCL 2.0.0
Distributed under the GNU Public License. See the file COPYING.
Dedicated to the memory of William Schelter.
The function bug_report() provides bug reporting information.
(%i1) quad_qag(sqrt(1+(16/25)*(1/y^2)),y,sqrt(8/5),8,1);
(%o1)          [6.94053457146499, 6.237015870261721e-11, 75, 0]
(%i2) quad_qag(sqrt(1+(16/25)*(1/y^2)),y,0.1,sqrt(8/5),1);
(%o2)         [2.434450712061476, 1.343848517124963e-10, 105, 0]
(%i3)
```

Figure 4.20: Cube Plot of Curve E

The total length of the arc is then the sum of both integrals, value equal to 9.37 mm. This value represents the minimum distance that the arc of the thermoformed sheet must have in order to clearly replicate the details of the designed pinheads. Therefore the relationship to be defined is as follows, where L is the total arc length and d is horizontal distance between the two pins which was defined as 10 mm for this calculation.

$$Factor = \frac{L}{d} = \frac{9.37}{10} = 0.937 \tag{4.9}$$

The value of 0.937, showed as result of equation 4.9, represents the factor by which the arc depth should be multiplied to calculate the minimum distance between consecutive pins in order not to lose details caused by drafts at the corners of the pinheads.

To verify if this theoretical value is valid, it is compared against the experimental 2(b) data gained from Curve E and is compared against sections 0, 1 and 10 as shown in figure 4.21.

The maximum value of arc length between consecutive pins was defined through experimental data. Values were taken from experiment 2(b). The table 4.2 presents the arc length and the distance between pins belonging to the E curve in different sections.

Those values in which the factor has a maximum value of 1.05 are the ones that present the best definition and the highest number of marked corners in the thermoformed plastic sheets. Then, factor 1.05 is presented as the maximum value of the ratio between the arc length and distance of consecutive pins, to attain the best surface quality in the current ex-

Table 4.2: Arc Length & Distance Ratio

Curve	Section	Pin Position x	Pin Position x+1	Pin Edges x	Pin Edges x+1	Pin Distance (mm)	Angle (°)	Arc Length (mm)	Factor Arc Length/ Pin Dstance
E	1	G	E	6	6	13	4.93	13.10	1.01
		E	C	6	6	13	13.75	13.73	1.06
		C	B	6	4	3	19.63	3.83	1.28
		B	A	4	3	3	24.51	4.28	1.43
	1	G	E	6	6	13	4.93	13.10	1.01
		E	C	6	6	13	13.75	13.73	1.06
		C	B	6	4	3	19.63	3.83	1.28
		B	A	4	3	3	24.05	4.28	1.43
	0	G	F	6	6	3	2.05	3.10	1.03
		F	E	6	5	3	6.98	3.10	1.03
		E	D	5	4	3	11.13	3.26	1.09
		D	C	4	6	3	15.34	3.49	1.16
		C	B	6	3	3	19.63	3.83	1.28
		B	A	3	4	3	24.51	4.33	1.44
	0	G	F	6	5	3	2.05	3.12	1.04
		F	E	5	4	3	6.98	3.50	1.17
		E	D	4	3	3	11.13	3.26	1.09
		D	C	3	3	3	15.34	3.49	1.16
		C	B	3	1	3	19.63	3.83	1.28
		B	A	1	3	3	24.51	4.33	1.44
	6	G	J	6	6	23	7.02	25.60	1.11
		J	M	6	6	23	19.75	27.88	1.21
	10	G	I	6	6	13	4.93	14.44	1.11
		I	J	6	4	3	11.13	3.40	1.13
		J	M	4	6	23	19.78	29.29	1.27

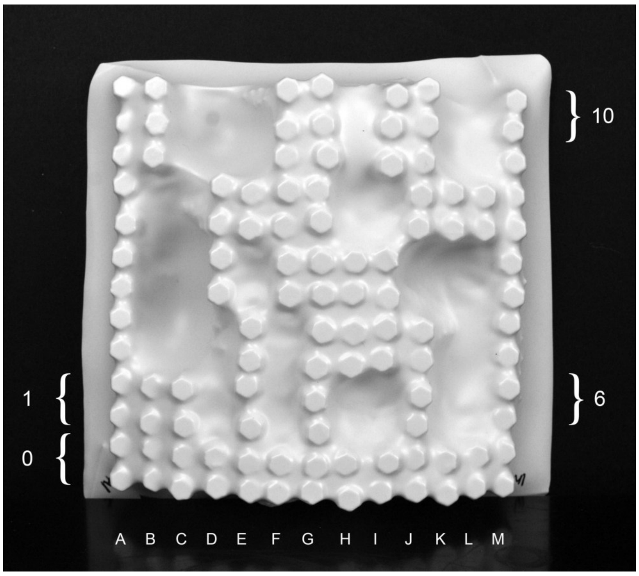

Figure 4.21: Curve E with configuration SHYP

perimental conditions. Two phenomena occur where those values that are above this factor:

- the number of corners that are reproduced decreased in the pin located at position x+1. This is explained by the proximity of this pin with its predecessor which limits the number of contact points between the plastic sheet and the pin head. Replicating the case showed in figure 4.17a.
- areas of structural support failure were identified in the thermoformed part. The phenomenon was associated with the reduction in sheet thickness evidenced by marked changes in the curve trajectory, replicating the case shown in figure 4.17c.

With this data, the values of height and distance between consecutive pins can be evaluated to verify if the relationship is between 0.937-1.05 in order to increase the details reproduced in the thermoformed film.

5 Conclusion

5.1 Conclusions

In this thesis the hypothesis that reconfigurable pin mould can create recognisable textures is studied. It is determined that the resolution of a reconfigurable pin mould is a key factor in producing details of a certain size and spacing. Therefore, applications in which details are required need to be defined before the manufacturing of the prototype.

The results indicate that geometric features presented different levels of definition. Flat sections delivered the most uniform definition, followed by concave sections and then convex sections. The highest level of definition is achieved with 10% incline which slowly decreases as incline degree is increased. The rendering of a geometric feature is directly proportional to the height and quantity of the contact points with the sheet.

The bed should be designed with each pins surrounded by equivalent number of vacuum holes and have ejector pins located at the edges of the mould to help with the demoulding. According to the best results, the best configuration to get detailed definition, the pins should be placed in a square grid and used with an interlayer.

The curve itself should be actuated on the reconfigurable pin mould in such a way, that the side with maximum projections is facing upwards. The shape of the pinhead is not a significant factor, however the distance between two pin heads must be within a specific range of minimum and maximum distance that can be defined between the range of 0.937-1.05 with respect to the height of the adjacent pin.

5.2 Future Works

The future research directions identified include:

- Testing the applications by casting silicon or plaster of paris into a vacuum-formed plastic mold and analyse the details transferred in the casting process.
- Use Micro QR code to encode information and then actuate it in the bed to tests it

readability by machines.

- Design organic pinheads for more aesthetic applications and test its translation with the desktop vacuum former. Also study its impact on human perception.
- Design a pinhead that can pivot to remain normal to the plastic sheet. It is important that the pivot can be scaled down while preserving its range of motion in both x and y axis.
- Study the influence of a combination of regular polygonal pinheads on surface quality by continuing the experimentation with different materials.
- Determining the optimal distance between the sheet and the pin tips for a controlled conformance.
- Process simulation by varying the input variables and determining the quality of the output surface. The simulations, if comparable with experimental results, can be used for different pin sizes, different materials, different sheet sizes, and different scales. The simulation will help reduce the number of experiments needed to arrive at the optimal set of parameters.
- A method to manage the pin placement, orientation, and removal as well as analyses of the life cycle and cost of the pins.
- Calculate the draw depth and wall thickness at each pin at the ideal distance.
- Study the effect of increase in part surface area in the formed sheet on the mechanical properties and optical properties.

5.3 Proposed Applications

According to the findings that have been proposed in this study, it is exhibited that reconfigurable pin moulds are able to produce, repeatable high definition details that can be rapidly changed by variating pinheads and y-axis position of the pins. Hence, the following list of sectors are suggested where the application of reconfigurable pin tooling technology might be relevant:

- Communication System - As previously mentioned, reconfigurable pin molds have been used as haptic and visual interfaces. Another advancement has been the development of soft tactile actuators and sensors that can be applied in virtual reality based environment to enhance the experience. [104]. Combining this technology with shape and size specific, reconfigurable pinheads in varied arrangement can create a 3D tactile and visual communication system that can aid in creating an inclusive and universal communication system for people with impaired vision. This system can also help mixed reality applications in the future.

- Artificial Landmark - The sheets formed with this method can be coded to record information. These 3d code will be useful in creating artificial landmarks that are machine readable and will aid in localization and navigation of mobile robots, autonomous vehicles and drones in harsh environments where 2D barcodes are unable to perform well due to being exposed to environment factors weather events such as rain, snow, fog, etc which can not only reduce the visibility and clarity of the images but also erode the information with time. These codes cannot be discarded, torn, obscured, wiped off, or easily degraded like QR codes. [105] [106] [107]
- Design Applications - In architectural sector, the surface texturing in single and double curves panels can be applied on a large scale in buildings. The ability to change pinheads with different shape and then arranging them into different tiling patterns, can create interesting façades for commercial installations.

Bibliography

[1] Francesco Gabriele Galizia et al. “The evolution of molds in manufacturing: from rigid to flexible”. In: *Procedia Manufacturing* 33 (2019), pp. 319–326.

[2] Ward Fleming. *Vertical three-dimensional image screen*. US Patent 4,654,989. Apr. 1987.

[3] Chris Munro and Daniel Walczyk. “Reconfigurable Pin-Type Tooling: A Survey of Prior Art and Reduction to Practice”. In: *Journal of Manufacturing Science and Engineering* 129.3 (Jan. 2007), pp. 551–565. ISSN: 1087-1357. DOI: 10.1115/1.2714577. eprint: https://asmedigitalcollection.asme.org/manufacturingscience/article-pdf/129/3/551/5567256/551_1.pdf. URL: https://doi.org/10.1115/1.2714577.

[4] Malcolm Gladwell. *The tipping point: How little things can make a big difference*. Little, Brown, 2006.

[5] Elsa Henriques, Paulo Pecas, and Pedro Filipe Cunha. “Perspectives of mould making industry for digital global manufacturing”. In: *Digital Enterprise Technology*. Springer, 2007, pp. 449–456.

[6] *adaptive moulds - Adapa - adaptive moulds*. Mar. 2021. URL: https://adapa.dk/.

[7] *Adaptive Tooling Technology for Agile R and D and Mass-Customization of Composite Parts - CIKONI - Innovate. Develop. Realize. Composite Engineering. Carbon Entwicklung - CFK (Carbon)*. Sept. 2018. URL: https://cikoni.com/en/adaptive-tooling-technology-for-mass-customization-of-composite-parts-and-fast-rd.

[8] Vijay Sarthy Mysore Sreedhara. “Control of thermoforming process parameters to manufacture surfaces with pin-based tooling”. PhD thesis. Clemson University, 2015.

[9] Gary Fredric Eigen. “Smoothing methods for discrete die forming”. PhD thesis. Massachusetts Institute of Technology, 1992.

[10] Troels H Pedersen and Torben A Lenau. “Variable geometry casting of concrete elements using pin-type tooling”. In: *Journal of manufacturing science and engineering* 132.6 (2010).

[11] Aditya Kelkar and Bahattin Koc. “Geometric planning and analysis for hybrid re-configurable molding and machining process”. In: *Rapid Prototyping Journal* (2008).

[12] Aditya Kelkar, Bahattin Koc, and Rakesh Nagi. "Rapidly re-configurable mold manufacturing of free-form objects". In: *International Design Engineering Technical Conferences and Computers and Information in Engineering Conference*. Vol. 37017. 2003, pp. 355–362.

[13] Aditya Kelkar, Rakesh Nagi, and Bahattin Koc. "Geometric algorithms for rapidly reconfigurable mold manufacturing of free-form objects". In: *Computer-Aided Design* 37.1 (2005), pp. 1–16.

[14] ZW Yin and YQ Xiong. "Geometric algorithms for direct integration of reverse engineering and rapidly reconfigurable mold manufacturing". In: *The International Journal of Advanced Manufacturing Technology* 56.5 (2011), pp. 721–727.

[15] A Kirby and LA Stauffer. "Analysis of pin characteristics for a variable geometry mold". In: *The International Journal of Advanced Manufacturing Technology* 32.7 (2007), pp. 698–704.

[16] Paul Bosscher and Imme Ebert-Uphoff. "Digital clay: Architecture designs for shape-generating mechanisms". In: *2003 IEEE International Conference on Robotics and Automation (Cat. No. 03CH37422)*. Vol. 1. IEEE. 2003, pp. 834–841.

[17] Benjamin J Peters. "Practical pin tooling". PhD thesis. Massachusetts Institute of Technology, 2013.

[18] Yong-Tai Im et al. "A comparison of pin actuation schemes for large-scale discrete dies". In: *Journal of Manufacturing Processes* 2.4 (2000), pp. 247–257.

[19] Jacques Berteau. *Variable-shape mold*. US Patent 5,330,343. July 1994.

[20] Naomasa NAKAJIMA. "A newly developed technique to fabricate complicated dies and electrodes with wires". In: *Bulletin of JSME* 12.54 (1969), pp. 1546–1554.

[21] Edwin Haas, Robert C Schwarz, and John M Papazian. "Design and test of a reconfigurable forming die". In: *Journal of Manufacturing processes* 4.1 (2002), pp. 77–85.

[22] Daniel F Walczyk and Yong-Tai Im. "A hydraulically-actuated reconfigurable tool for flexible fabrication: implementation and control". In: *J. Manuf. Sci. Eng.* 122.3 (2000), pp. 562–568.

[23] David H Humphrey. *Mold forming device*. US Patent 3,596,869. Mar. 1971.

[24] Alvaro Paul et al. "Robotic manufacturing of near-net-shape components utilizing stereo imaging and reconfigurable tooling". In: *The International Journal of Advanced Manufacturing Technology* 63.9-12 (2012), pp. 999–1009.

[25] Masaaki Todoroki et al. *Apparatus and method for producing variable configuration die*. US Patent 5,253,176. Oct. 1993.

[26] Stephen G Kaufman and Barry L Spletzer. *Methods for freeform fabrication of structures*. US Patent 6,080,343. June 2000.

[27] Junichi Yamaoka and Yasuaki Kakehi. "ProtoMold: An interactive vacuum forming system for rapid prototyping". In: *Proceedings of the 2017 CHI Conference on Human Factors in Computing Systems*. 2017, pp. 2106–2115.

[28] John Cochrane. *Improvement in presses for bending metallic plates*. US Patent 39,886A. Sept. 1863.

[29] George T Pinson. *Apparatus for forming sheet metal*. US Patent 4,212,188. July 1980.

[30] Jerrell A Nardiello, Robert J Christ, and John M Papazian. *Block-set form die assembly*. US Patent 6,053,026. Apr. 2000.

[31] EW Ansted. *Machine for bending and forming springs*. US Patent US483094A. 1892.

[32] Charles P Trudell. *Sheet metal forming apparatus*. US Patent 2,280,359. Feb. 1942.

[33] Daniel F Walczyk, Jayant Lakshmikanthan, and Daniel R Kirk. "Development of a reconfigurable tool for forming aircraft body panels". In: *Journal of Manufacturing Systems* 17.4 (1998), pp. 287–296.

[34] HS Kleespies III and RH Crawford. "Vacuum forming of compound curved surfaces with a variable geometry mold". In: *Journal of manufacturing systems* 17.5 (1998), pp. 325–337.

[35] HR Schipper et al. "Optimization of the flexible mould process for the production of double-curved concrete elements". In: *CIC 2014: The 1st Concrete Innovation Conference, Oslo, Norway* (2014).

[36] ADC Pronk, T Lusing, and RHPG Versteeg. "The VaCo Mould, a new moulding technique for fluid architecture". In: *Proceedings of IASS Annual Symposia*. Vol. 2015. 1. International Association for Shell and Spatial Structures (IASS). 2015, pp. 1–9.

[37] Judah Hook. "Automated digital fabrication concept for composite facades". MA thesis. The University of Queensland, 2016.

[38] Kihong Ku and Satpal Gurjar. "Prototyping Method for Complex-Shaped Textile Composite Panels-Developing a digitally controlled reconfigurable mold". In: *Computing for a better tomorrow - Proceedings of the 36th eCAADe Conference - Volume 2, Lodz University of Technology, Lodz, Poland, 19-21 September 2018, pp. 47-52* (2018).

[39] C Raun and PH Kirkegaard. "Adaptive mould-A cost-effective mould system linking design and manufacturing of double-curved GFRC panels". In: *17th international congress of GRCA-GRC, Dubai*. 2015.

[40] ADC Pronk et al. "Flexible mould by the use of spring steel mesh". In: *Proceedings of IASS Annual Symposia*. Vol. 2015. 29. International Association for Shell and Spatial Structures (IASS). 2015, pp. 1–9.

[41] Ghang Lee and Seonwoo Kim. "Case study of mass customization of double-curved metal façade panels using a new hybrid sheet metal processing technique". In: *Journal of Construction Engineering and Management* 138.11 (2012), pp. 1322–1330.

[42] Rachel M Narciso. "Design of a rapidly reconfigurable pin-type molding device for near-net shape solid object generation". MA thesis. Purdue University, 2011.

[43] Michael F Zäh, Florian Hagemann, and Stefan Teufelhart. "Form-flexible tools for injection molding: approach for the economic application of injection molding for small lot sizes". In: *Production Engineering* 3.3 (2009), pp. 281–285.

[44] Bahattin Koc and Sridhar Thangaswamy. “Design and analysis of a reconfigurable discrete pin tooling system for molding of three-dimensional free-form objects”. In: *Robotics and Computer-Integrated Manufacturing* 27.2 (2011), pp. 335–348.

[45] Kuo-Fui Hong. *Molding mechanism*. US Patent 5,281,117. Jan. 1994.

[46] Marie Jonsson and Gilbert Ossbahr. “Aspects of reconfigurable and flexible fixtures”. In: *Production Engineering* 4.4 (2010), pp. 333–339.

[47] Jin Woo Park et al. “Assembly Part Positioning on Transformable Pin Array Fixture by Active Pin Maximization and Joining Point Alignment”. In: *IEEE Transactions on Automation Science and Engineering* (2021).

[48] Hiroo Iwata et al. “Project FEELEX: adding haptic surface to graphics”. In: *Proceedings of the 28th annual conference on Computer graphics and interactive techniques*. 2001, pp. 469–476.

[49] Alexa F Siu et al. “shapeCAD: An accessible 3D modelling workflow for the blind and visually-impaired via 2.5 D shape displays”. In: *The 21st International ACM SIGACCESS Conference on Computers and Accessibility*. 2019, pp. 342–354.

[50] Sean Follmer et al. “inFORM: dynamic physical affordances and constraints through shape and object actuation.” In: *Uist*. Vol. 13. 10.1145. 2013, pp. 2501988–2502032.

[51] Alexa F Siu et al. “Shapeshift: 2D spatial manipulation and self-actuation of tabletop shape displays for tangible and haptic interaction”. In: *Proceedings of the 2018 CHI Conference on Human Factors in Computing Systems*. 2018, pp. 1–13.

[52] Ryo Suzuki et al. “LiftTiles: constructive building blocks for prototyping room-scale shape-changing interfaces”. In: *Proceedings of the Fourteenth International Conference on Tangible, Embedded, and Embodied Interaction*. 2020, pp. 143–151.

[53] Hiroshi Ishii et al. “TRANSFORM: Embodiment of" Radical Atoms" at Milano Design Week”. In: *Proceedings of the 33rd Annual ACM Conference Extended Abstracts on Human Factors in Computing Systems*. 2015, pp. 687–694.

[54] Luke Vink et al. “Transform as adaptive and dynamic furniture”. In: *Proceedings of the 33rd Annual ACM Conference Extended Abstracts on Human Factors in Computing Systems*. 2015, pp. 183–183.

[55] Aubrey Colter et al. “SoundFORMS: Manipulating sound through touch”. In: *Proceedings of the 2016 CHI Conference Extended Abstracts on Human Factors in Computing Systems*. 2016, pp. 2425–2430.

[56] Jarek Rossignac et al. “Finger sculpting with digital clay: 3d shape input and output through a computer-controlled real surface”. In: *2003 Shape Modeling International.* IEEE. 2003, pp. 229–231.

[57] Haihong Zhu and Wayne J Book. “Practical structure design and control for digital clay”. In: *ASME International Mechanical Engineering Congress and Exposition*. Vol. 47063. 2004, pp. 1051–1058.

[58] KW Tam and KW Chan. “Thermoforming mould design using a reverse engineering approach”. In: *Robotics and Computer-Integrated Manufacturing* 23.3 (2007), pp. 305–314.

[59] Nikolaj Kjelgaard Vedel-Smith and Torben Anker Lenau. “Casting traceability with direct part marking using reconfigurable pin-type tooling based on paraffin–graphite actuators”. In: *Journal of Manufacturing Systems* 31.2 (2012), pp. 113–120.

[60] Zhijian Wang. “Rapid manufacturing of vacuum forming components utilising reconfigurable screw pin tooling”. PhD thesis. University of Nottingham, 2010.

[61] Dominik Simon et al. “A reconfigurable tooling system for producing plastic shields”. In: *Procedia CIRP* 17 (2014), pp. 853–858.

[62] Daniel F Walczyk, Jean F Hosford, and John M Papazian. “Using reconfigurable tooling and surface heating for incremental forming of composite aircraft parts”. In: *J. Manuf. Sci. Eng.* 125.2 (2003), pp. 333–343.

[63] Syed Ali Ashter. *Thermoforming of Single and Multilayer Laminates: Plastic Films Technologies, Testing, and Applications*. William Andrew, 2013.

[64] James L Throne. *Understanding thermoforming*. Hanser Gardner Publications OH, 2008.

[65] Peter Klein. “Fundamentals of plastics thermoforming”. In: *Synthesis Lectures on Materials Engineering* 1.1 (2009), pp. 1–97.

[66] Hollee Keller. *It’s time to update our thermoformers’ ranking*. Feb. 2020. URL: https://www.plasticsnews.com/blog/its-time-update-our-thermoformers-ranking.

[67] Nancy D Lamontagne. “Green Thermoforming: Materials suppliers and converters embrace biobased options to meet market demands for sustainable products”. In: *Plastics Engineering* 76.8 (2020), pp. 36–39.

[68] Huidong Wei. “Optimisation on thermoforming of biodegradable poly (lactic acid)(PLA) by numerical modelling”. In: *Polymers* 13.4 (2021), p. 654.

[69] M Barletta and M Puopolo. “Thermoforming of compostable PLA/PBS blends reinforced with highly hygroscopic calcium carbonate”. In: *Journal of Manufacturing Processes* 56 (2020), pp. 1185–1192.

[70] Fouad Erchiqui and Mhamed Souli. “Numerical investigation on the use of wood–plastic composites for the thermoforming of NACA profile for UAVs”. In: *Multiphysics Simulations in Automotive and Aerospace Applications*. Elsevier, 2021, pp. 209–238.

[71] Ashir Mittal et al. *Designing a Production-Ready Ultra-Lightweight Carbon Fiber Reinforced Thermoplastic Composites Door*. Tech. rep. SAE Technical Paper, 2021.

[72] Robert M Stack and Francis Lai. “Development in thermoforming thermoplastic composites”. In: *Thermoforming Quarterly* 32 (2013), pp. 48–53.

[73] Hyun-Joong Lee, Dong-Ju Shin, and Keun Park. “Ultrasonic thermoforming of a large thermoplastic polyurethane film with the aid of infrared heating”. In: *Journal of Mechanical Science and Technology* 31.12 (2017), pp. 5687–5693.

[74] Stanley R Rosen. *Thermoforming: improving process performance*. Society of Manufacturing Engineers, 2002.

[75] Mark Kishel. *Changing texture is easy with Thermoformed Plastic Parts*. July 2018. URL: https://www.arrowheadinc.com/advantage-using-textures-thermoformed-plastic-parts/.

[76] George Gruenwald. *Thermoforming: a plastics processing guide*. Routledge, 2018.

[77] Serge Pacome Kaho et al. "Development of a Composite Material Based on Wood Waste Stabilized with Recycled Expanded Polystyrene". In: *Open Journal of Composite Materials* 10.03 (2020), p. 66.

[78] K Sanguanwong et al. "Polymeric feedstock from post-consumer and post-industrial plastic wastes for automotive interior applications". In: *IOP Conference Series: Materials Science and Engineering*. Vol. 455. 1. IOP Publishing. 2018, p. 012048.

[79] PO Awoyera and Adeyemi Adesina. "Plastic wastes to construction products: Status, limitations and future perspective". In: *Case Studies in Construction Materials* 12 (2020), e00330.

[80] Sven Engelmann. *Advanced thermoforming: methods, machines and materials, applications and automation*. Vol. 8. John Wiley & Sons, 2012.

[81] Tahir Altınbalık et al. "Thermoforming of Biopolymer-Green Polyethylene Sheets". In: *International Journal of Modern Manufacturing Technologies, ISSN 2067–3604, Vol. X, No. 2* (2018).

[82] Daniela G Coblas et al. "Manufacturing textured surfaces: State of art and recent developments". In: *Proceedings of the institution of mechanical engineers, Part J: Journal of Engineering Tribology* 229.1 (2015), pp. 3–29.

[83] Nobuyuki Moronuki. "Functional texture design and texturing processes". In: *International journal of automation technology* 10.1 (2016), pp. 4–15.

[84] Yannick Joye. "Architectural lessons from environmental psychology: The case of biophilic architecture". In: *Review of general psychology* 11.4 (2007), pp. 305–328.

[85] Malcolm Innes. *Lighting for interior design*. Hachette UK, 2012.

[86] Charles Spence. "Tactile/haptic aspects of multisensory packaging design". In: *Multisensory Packaging*. Springer, 2019, pp. 127–159.

[87] Bruno M Ferreira. "Packaging texture influences product taste and consumer satisfaction". In: *Journal of Sensory Studies* 34.6 (2019), e12532.

[88] Maria Lilian de Araújo Barbosa et al. "Accessible Packaging: a study for inclusive models for visual impairment people". In: *International Conference on Applied Human Factors and Ergonomics*. Springer. 2018, pp. 282–292.

[89] Gisele Yumi Arabori Ribeiro et al. "Information for Tactile Reading: A Study of Tactile Ergonomics of Packaging for Blind People". In: *Congress of the International Ergonomics Association*. Springer. 2018, pp. 1682–1688.

[90] Alina Surmacka Szczesniak. “Texture is a sensory property”. In: *Food quality and preference* 13.4 (2002), pp. 215–225.

[91] Malcolm Bourne. *Food texture and viscosity: concept and measurement*. Elsevier, 2002.

[92] J Chen and A Rosenthal. “Food texture and structure”. In: *Modifying food texture*. Elsevier, 2015, pp. 3–24.

[93] Sirada Sungsinchai et al. “Texture modification technologies and their opportunities for the production of dysphagia foods: A review”. In: *Comprehensive reviews in food science and food safety* 18.6 (2019), pp. 1898–1912.

[94] Chantal Nederkoorn et al. “Taste the feeling or feel the tasting: Tactile exposure to food texture promotes food acceptance”. In: *Appetite* 120 (2018), pp. 297–301.

[95] Jay T Worobets et al. “Increasing running shoe traction can enhance performance”. In: *Research Journal of Textile and Apparel* (2014).

[96] Christine Hovliaras et al. “Ergonomics and Toothbrushes”. In: *The Journal of clinical dentistry* 26.1 (2015), pp. 28–32.

[97] Lucia Rodriguez-Parada, Pedro F Mayuet, and Antonio J Gámez. “Evaluation of Reliefs’ Properties on Design of Thermoformed Packaging Using Fused Deposition Modelling Moulds”. In: *Materials* 12.3 (2019), p. 478.

[98] Lucia Rodriguez Parada, Pedro Ares, and Rafael Bienvenido. “Food Packaging Design. Case of Study about perception of shapes and reliefs thermoformed”. In: *Tools and Methods of Competitive Engineering At: Las Palmas de Gran Canaria* (May 2018).

[99] Maggie Macnab. *Design by nature : using universal forms and principles in design*. Berkeley, CA: New Riders, 2012. ISBN: 978-0321747761.

[100] Lewis F Day. *Pattern design*. Courier Corporation, 2013.

[101] Robert Fathauer. *Tessellations: Mathematics, Art, and Recreation*. CRC Press, 2020.

[102] Yan Wang, Z-J Wang, and Nabil Gindy. “A method for representation of component geometry using discrete pin for reconfigurable moulds”. In: *Advances in Engineering Software* 42.7 (2011), pp. 409–418.

[103] Mohammad Ghobadnam et al. “Numerical and experimental analysis of HIPS sheets in thermoforming process”. In: *The International Journal of Advanced Manufacturing Technology* 76.5-8 (2015), pp. 1079–1089.

[104] Phone May Khin et al. “Soft haptics using soft actuator and soft sensor”. In: *2016 6th IEEE International Conference on Biomedical Robotics and Biomechatronics (BioRob)*. IEEE. 2016, pp. 1272–1276.

[105] Feng Wen et al. “Visual navigation of an indoor mobile robot based on a novel artificial landmark system”. In: *2009 International Conference on Mechatronics and Automation*. IEEE. 2009, pp. 3775–3780.

[106] Bo Yi Li et al. "On 3D autonomous delivery systems: Design and development". In: *2017 International Conference on Advanced Robotics and Intelligent Systems (ARIS)*. IEEE. 2017, pp. 1–6.

[107] Christian Schüller et al. "Computational thermoforming". In: *ACM Transactions on Graphics (TOG)* 35.4 (2016), pp. 1–9.

Appendix

Appendix A

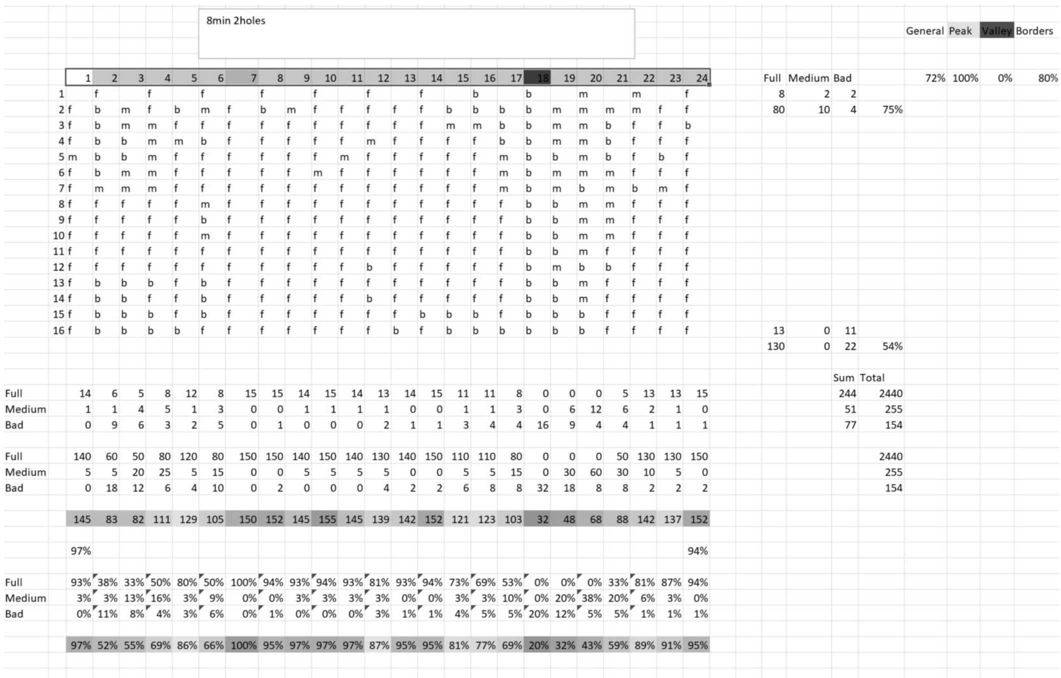

8min 2holes

		1	2	3	4	5	6	7	8	9	10	11	12	13	14	15	16	17	18	19	20	21	22	23	24
	1		f		f		f		f		f		f		f		b		b		m		m		f
	2	f	b	m	f	b	m	f	b	m	f	f	f	f	f	b	b	b	b	m	m	m	m	f	f
	3	f	b	m	m	f	f	f	f	f	f	f	f	f	f	m	m	b	b	m	m	b	f	f	b
	4	f	b	b	m	m	b	f	f	f	f	f	m	f	f	f	f	b	b	m	m	b	f	f	f
	5	m	b	b	m	f	f	f	f	f	f	m	f	f	f	f	f	m	b	b	m	b	f	b	f
	6	f	b	m	m	f	f	f	f	f	m	f	f	f	f	f	f	m	b	m	m	m	f	f	f
	7	f	m	m	m	f	f	f	f	f	f	f	f	f	f	f	f	m	b	m	b	m	b	m	f
	8	f	f	f	f	f	m	f	f	f	f	f	f	f	f	f	f	f	b	b	m	m	f	f	f
	9	f	f	f	f	f	b	f	f	f	f	f	f	f	f	f	f	f	b	b	m	m	f	f	f
	10	f	f	f	f	f	m	f	f	f	f	f	f	f	f	f	f	f	b	b	m	m	f	f	f
	11	f	f	f	f	f	f	f	f	f	f	f	f	f	f	f	f	f	b	b	m	f	f	f	f
	12	f	f	f	f	f	f	f	f	f	f	f	b	f	f	f	f	f	b	m	b	b	f	f	f
	13	f	b	b	b	f	b	f	f	f	f	f	f	f	f	f	f	f	b	b	m	f	f	f	f
	14	f	b	b	f	f	b	f	f	f	f	f	b	f	f	f	f	f	b	b	m	f	f	f	f
	15	f	b	b	b	f	b	f	f	f	f	f	f	f	b	b	b	f	b	b	b	f	f	f	f
	16	f	b	b	b	b	f	f	f	f	f	f	f	b	f	b	b	b	b	b	b	f	f	f	f
Full		14	6	5	8	12	8	15	15	14	15	14	13	14	15	11	11	8	0	0	0	5	13	13	15
Medium		1	1	4	5	1	3	0	0	1	1	1	1	0	0	1	1	3	0	6	12	6	2	1	0
Bad		0	9	6	3	2	5	0	1	0	0	0	2	1	1	3	4	4	16	9	4	4	1	1	1
Full		140	60	50	80	120	80	150	150	140	150	140	130	140	150	110	110	80	0	0	0	50	130	130	150
Medium		5	5	20	25	5	15	0	0	5	5	5	5	0	0	5	5	15	0	30	60	30	10	5	0
Bad		0	18	12	6	4	10	0	2	0	0	0	4	2	2	6	8	8	32	18	8	8	2	2	2
		145	83	82	111	129	105	150	152	145	155	145	139	142	152	121	123	103	32	48	68	88	142	137	152
		97%																							94%
Full		93%	38%	33%	50%	80%	50%	100%	94%	93%	94%	93%	81%	93%	94%	73%	69%	53%	0%	0%	0%	33%	81%	87%	94%
Medium		3%	3%	13%	16%	3%	9%	0%	0%	3%	3%	3%	3%	0%	0%	3%	3%	10%	0%	20%	38%	20%	6%	3%	0%
Bad		0%	11%	8%	4%	3%	6%	0%	1%	0%	0%	0%	3%	1%	1%	4%	5%	5%	20%	12%	5%	5%	1%	1%	1%
		97%	52%	55%	69%	86%	66%	100%	95%	97%	97%	97%	87%	95%	95%	81%	77%	69%	20%	32%	43%	59%	89%	91%	95%

General	Peak	Valley	Borders
72%	100%	0%	80%

Full	Medium	Bad	
8	2	2	
80	10	4	75%
13	0	11	
130	0	22	54%

Sum	Total
244	2440
51	255
77	154
	2440
	255
	154

Figure 5.1: Analysis of curve A4

Appendix B

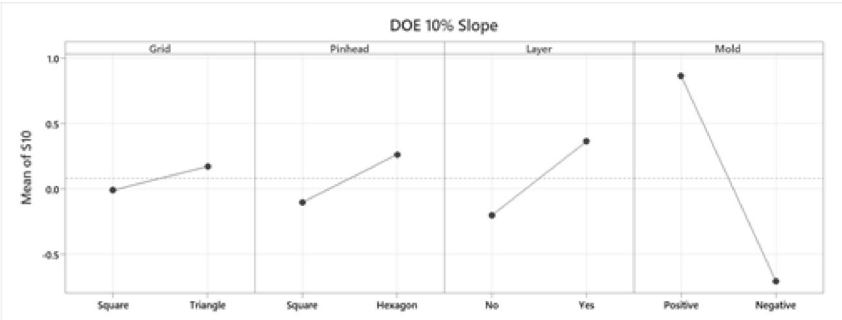

Figure 5.2: Doe of Slope with 10% Incline

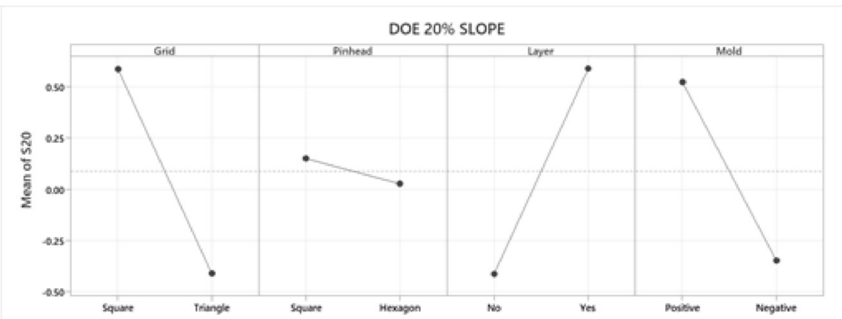

Figure 5.3: Doe of Slope with 20% Incline

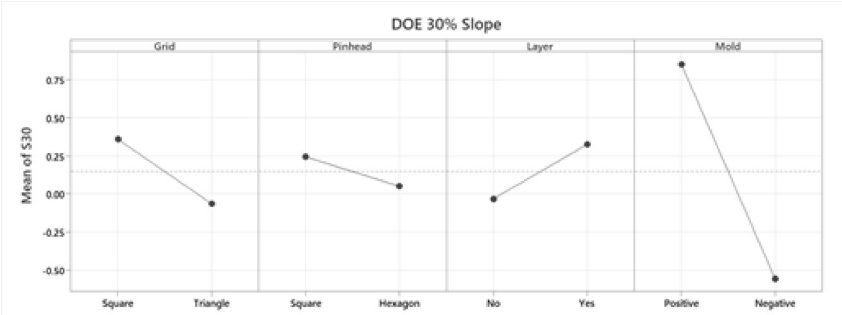

Figure 5.4: Doe of Slope with 30% Incline

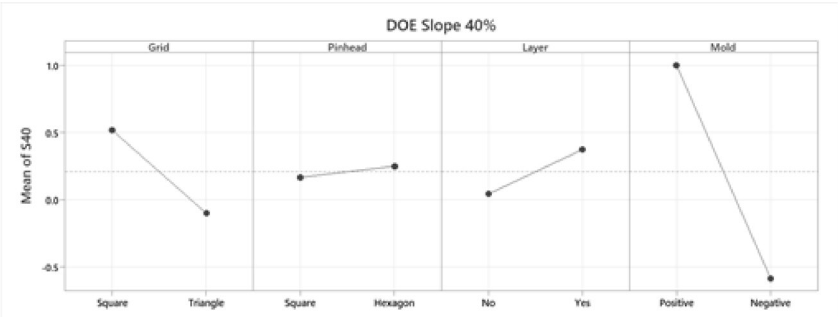

Figure 5.5: Doe of Slope with 40% Incline

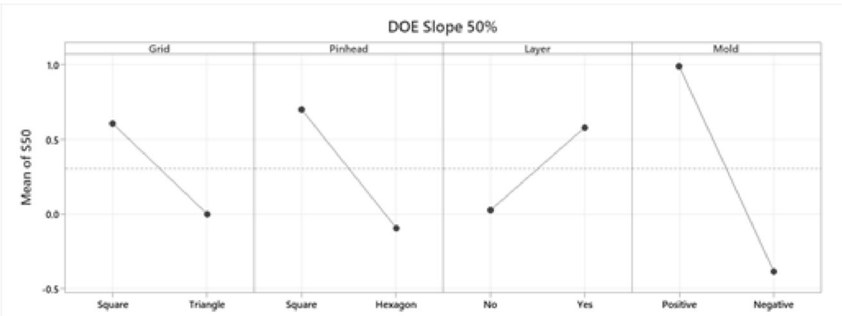

Figure 5.6: Doe of Slope with 50% Incline

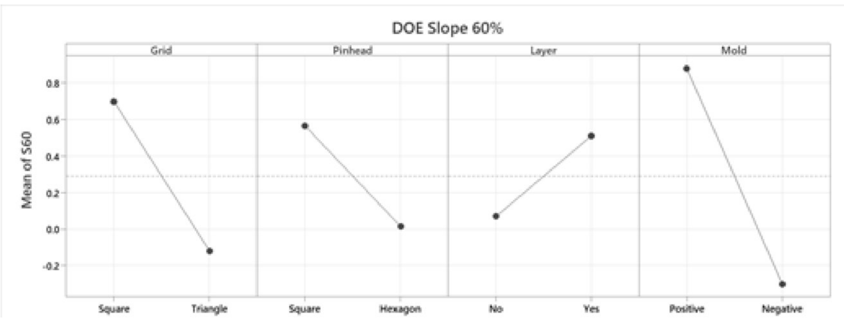

Figure 5.7: Doe of Slope with 60% Incline

Appendix C

CURVE D	SLOPE		10%	20%	30%	40%	50%	Slope 60%	Average
		mean	0.751	0.602	0.508	0.363	0.228	0.207	0.472
Configuration		std	0.114	0.113	0.161	0.183	0.144	0.133	0.128
SSNP			1.178	1.107	0.860	0.918	1.457	1.270	1.102
SSYN			-0.836	0.204	-0.308	-0.275	0.154	0.328	-0.283
TSNN			-1.476	-0.698	0.211	-0.275	0.154	0.328	-0.369
SHYP			0.842	2.043	2.200	2.338	1.891	2.212	2.105
SHNN			-1.232	-1.012	-1.322	-0.919	-1.087	-1.023	-1.329
THYN			0.720	0.119	-0.803	-0.869	-0.756	-0.835	-0.563
TSYP			0.720	-0.016	0.211	0.293	1.023	0.328	0.419
THNP			0.720	-1.046	0.125	0.444	-0.425	-0.301	-0.081

Figure 5.8: Matrix values evaluation: Experiment 2 a)

CURVE E	ARCH		1	2	3	4	5	6	7	8	9	10	Average
		mean	1.771	0.397	0.477	0.545	0.276	0.524	0.586	0.429	0.747	0.774	0.573
Configuration		std	0.861	0.543	0.444	0.310	0.349	0.786	0.708	0.495	0.711	0.983	0.789
SSNP			0.205	-0.229	-0.306	-0.719	-0.144	0.039	-0.347	-0.265	-0.316	-0.408	-0.068
SSYN			0.685	-0.315	-0.431	0.316	-0.033	-0.183	-0.145	-0.194	-0.089	0.103	0.102
TSNN			-1.274	-0.416	-0.590	-0.963	-0.107	-0.422	-0.432	-0.375	-0.349	-0.547	-0.347
SHYP			2.007	2.780	2.217	2.115	2.861	1.612	2.441	2.116	2.312	0.993	1.690
SHNN			-1.114	-0.105	-0.318	-0.808	-0.476	-0.554	-0.533	-0.574	-0.861	-0.530	-0.382
THYN			0.118	0.668	1.550	1.167	-0.157	0.550	0.290	0.111	1.007	0.512	0.528
TSYP			0.685	-0.315	-0.431	0.316	-0.033	-0.183	-0.145	-0.194	-0.089	0.103	0.102
THNP			0.829	0.240	0.691	0.628	0.037	2.428	1.474	1.926	1.318	2.649	1.217

Figure 5.9: Matrix values evaluation: Experiment 2 b)